

1 **Air-sea CO₂ fluxes in the East China Sea based on**
2 **multiple-year underway observations**

3 **X.-H. Guo¹, W.-D. Zhai^{1,2}, M.-H. Dai¹, *, C. Zhang¹, Y. Bai³, Y. Xu¹, Q. Li¹,**
4 **G.-Z. Wang¹**

5 [1] {State Key Laboratory of Marine Environmental Science, Xiamen University,
6 Xiamen 361102, China

7 [2] {National Environmental Monitoring Center, Dalian 116023, China }

8 [3] {State Key Laboratory of Satellite Ocean Environment Dynamics, Second
9 Institute of Oceanography, State Oceanic Administration, Hangzhou 310012, China }

10

11

12 Correspondence to: M.-H. Dai (mdai@xmu.edu.cn)

13

14

15 **Abstract**

16 This study reports thus far a most comprehensive dataset of surface seawater $p\text{CO}_2$
17 (partial pressure of CO_2) and the associated air-sea CO_2 fluxes in a major ocean
18 margin, the East China Sea (ECS) based on 24 surveys conducted in 2006 to 2011. We
19 showed highly dynamic spatial variability of sea surface $p\text{CO}_2$ in the ECS except in
20 winter when it ranged in a narrow band of 330 to 360 μatm . We categorized the ECS
21 into five different domains featured with different physics and biogeochemistry to
22 better characterize the seasonality of the $p\text{CO}_2$ dynamics and to better constrain the
23 CO_2 flux. The five domains are (I) the outer Changjiang estuary and Changjiang
24 plume, (II) the Zhejiang-Fujian coast, (III) the northern ECS shelf, (IV) the middle
25 ECS shelf, and (V) the southern ECS shelf. In spring and summer, $p\text{CO}_2$ off the
26 Changjiang estuary was as low as $<100 \mu\text{atm}$, while it was up to $>400 \mu\text{atm}$ in fall.
27 $p\text{CO}_2$ along the Zhejiang-Fujian coast was low in spring, summer and winter (300 to
28 350 μatm) but was relatively high in fall ($>350 \mu\text{atm}$). In the northern ECS shelf,
29 $p\text{CO}_2$ in summer and fall was $>340 \mu\text{atm}$ in most areas, higher than in winter and
30 spring. In the middle and southern ECS shelf, $p\text{CO}_2$ in summer ranged from 380 to
31 400 μatm , which was higher than in other seasons ($<350 \mu\text{atm}$). The area-weighted
32 CO_2 flux in the entire ECS shelf was $-10.0 \pm 2.0 \text{ mmol m}^{-2} \text{ d}^{-1}$ in winter, -11.7 ± 3.6
33 $\text{mmol m}^{-2} \text{ d}^{-1}$ in spring, $-3.5 \pm 4.6 \text{ mmol m}^{-2} \text{ d}^{-1}$ in summer and $-2.3 \pm 3.1 \text{ mmol m}^{-2} \text{ d}^{-1}$
34 in fall. It is important to note that the standard deviations in these flux ranges mostly
35 reflect the spatial variation of $p\text{CO}_2$ rather than the bulk uncertainty. Nevertheless, on
36 an annual basis, the average CO_2 influx into the entire ECS shelf was $6.9 \pm 4.0 \text{ mmol}$
37 $\text{m}^{-2} \text{ d}^{-1}$, about twice the global average in ocean margins.

38 **1 Introduction**

39 With the rapid growth of carbon flux measurements during the past decade, our
40 estimation of the coastal ocean air-sea CO_2 fluxes have converged to about 0.2 to 0.5
41 Pg C yr^{-1} at a global scale (Borges et al., 2005; Cai et al., 2006; Chen and Borges,
42 2009; Chen et al., 2013; Dai et al., 2013; Laruelle et al., 2010; Laruelle et al., 2014)

43 and it is safe to state that the earlier estimate of up to 0.9 to 1.0 Pg C yr⁻¹ was an
44 overestimate. Having stated so, it remains, however, challenging to reliably assess the
45 carbon fluxes in individual coastal systems that are often featured by the greatest
46 spatial and temporal variations (Cai and Dai, 2004; Dai et al., 2013; Dai et al., 2009;
47 Zhai et al., 2013). Understanding regional fluxes and controls is important because it
48 would not only affect global flux estimation, but also improve our capability of
49 modeling the coastal ocean carbon cycle. A regional climate model that is particularly
50 relevant to the societal sustainability would need an improved estimate of regional
51 carbon fluxes to resolve its predictability of future changes. Finally, many coastal
52 oceans have been impacted by anthropogenic activities, the signals of which remains
53 however challenging to decipher (Chou et al., 2007; Omar et al., 2003).

54 The East China Sea (ECS) is a shelf system characterized by significant terrestrial
55 input from a major world river from the west, the Changjiang (Yangtze River), as well
56 as dynamic exchange at its eastern board with the Kuroshio, a major western ocean
57 boundary current (Chen and Wang, 1999). Located in the temperate zone, the ECS is
58 also characterized by a clear seasonal pattern with warm and productive summer, and
59 cold and less productive winter (Gong et al., 2003; Han et al., 2013). Such a dynamic
60 nature in both physical circulation and biogeochemistry makes for large contrasts in
61 different zones within the ECS and thus zonal based assessment is critical to reliably
62 constrain the CO₂ flux in time and space in this important marginal sea.

63 Prior studies already reveal that the ECS is overall an annual net sink of the
64 atmospheric CO₂ with significant seasonal variations (Chou et al., 2009; Chou et al.,
65 2011; Kim et al., 2013; Peng et al., 1999; Shim et al., 2007; Tseng et al., 2011;
66 Tsunogai et al., 1999; Wang et al., 2000; Zhai and Dai, 2009). The ranges of present
67 estimates are -3.3 to -6.5 mmol m⁻² d⁻¹ in spring, -2.4 to -4.8 mmol m⁻² d⁻¹ in summer,
68 0.4 to 2.9 mmol m⁻² d⁻¹ in fall and -13.7 to -10.4 mmol m⁻² d⁻¹ in winter. However,
69 these estimates are either based on limited (only one or a few) field surveys (Chou et
70 al., 2009; Chou et al., 2011; Peng et al., 1999; Shim et al., 2007; Tsunogai et al., 1999;

71 Wang et al., 2000) or suffer from spatial limitation (Kim et al., 2013; Shim et al., 2007;
72 Tsunogai et al., 1999; Zhai and Dai, 2009). Tseng et al. (2011) investigate the
73 Changjiang Dilution Water induced CO₂ uptake in summer and obtain an empirical
74 algorithm of surface water *p*CO₂ (partial pressure of CO₂) with the Changjiang
75 discharge and sea surface temperature (SST). Subsequently, they extrapolate the
76 empirical algorithm to the entire ECS shelf and the whole year to obtain a significant
77 CO₂ sink of 6.3±1.1 mmol m⁻² d⁻¹ (Tseng et al., 2011). With data from three field
78 surveys conducted in spring, fall and winter added, Tseng et al. (2014) update the
79 annual CO₂ flux in the ECS to be -4.9±1.4 mmol m⁻² d⁻¹ using the similar empirical
80 algorithm method.

81 In this study, we investigated the air-sea CO₂ fluxes on the entire ECS shelf based on
82 large scale observations of 24 mapping cruises from 2006 to 2011, resolving both
83 spatial coverage and fully seasonal variations. This largest dataset, thus far, allowed
84 for a better constraint of the carbon fluxes in this important ocean margin system. The
85 estimate in an individual survey was based on the gridded average values in five
86 physically and biogeochemically distinct domains (Fig. 1), based on which, the
87 distribution of the *p*CO₂ and the major controls in the ECS were better revealed, and
88 the air-sea CO₂ fluxes were better estimated.

89 **2 Study area**

90 The ECS is one of the major marginal seas located in the western Pacific. The largest
91 freshwater source to the ECS is the Changjiang, which delivers 940 km^3 freshwater
92 annually with the highest discharge in summer (Dai and Trenberth, 2002). The
93 circulation of the ECS is modulated by the East Asian monsoon. The northeast winds
94 in winter last from September to April and the summer monsoon from the southwest
95 is weaker and lasts from July to August. The Changjiang plume flows northeastward
96 in summer but southwestward along the China coastline in winter (Lee and Chao,
97 2003). The northward flowing Kuroshio follows the isobaths beyond the shelf break
98 at $\sim 200 \text{ m}$ (Lee and Chao, 2003; Liu and Gan, 2012). Near the shelf break, there are
99 upwellings centered at the northeast of Taiwan Island and the southwest of Kyushu
100 Island (Lee and Chao, 2003).

101 The SST in the ECS is low in winter and early spring but high in summer and early
102 fall. The seasonal variation in SST is up to $10 \text{ }^\circ\text{C}$ in the inner shelf and $\sim 5 \text{ }^\circ\text{C}$ in the
103 outer shelf (Gong et al., 2003). In warm seasons, productivity in the ECS is as high
104 as $>1 \text{ g C m}^{-2} \text{ d}^{-1}$ (Gong et al., 2003). Changjiang freshwater and the upwelling of the
105 Kuroshio subsurface water are believed to be the major sources of nutrients to the
106 ECS shelf (Chen and Wang, 1999). Regulated by both productivity and temperature,
107 $p\text{CO}_2$ shows strong seasonal variations, typically under-saturated in cold seasons and
108 in productive areas in warm seasons (Chou et al., 2009; Chou et al., 2011; Tseng et al.,
109 2011).

110 We categorized the ECS shelf into five distinct domains featured by different
111 physical-biogeochemical characteristics based on the distributions of SST, chlorophyll
112 a (Chl- a) concentrations and turbidity (Fig. 1). The boundaries, surface areas and
113 characteristics of the five domains are presented in Table 1 and Fig. 1. Domains I
114 ($28.5\text{-}33.0 \text{ }^\circ\text{N}$, $122.0\text{-}126.0 \text{ }^\circ\text{E}$, $191 \times 10^3 \text{ km}^2$) and II ($25.0\text{-}28.5 \text{ }^\circ\text{N}$, $119.3\text{-}123.5 \text{ }^\circ\text{E}$,
115 $41 \times 10^3 \text{ km}^2$) are essentially in the inner shelf shallower than 50 m . Domain I, being
116 the core area of the outer Changjiang estuary and the near field Changjiang plume in

117 warm seasons, is characterized by high Chl-*a* (He et al., 2013) and lowest $p\text{CO}_2$ in
118 warm seasons (Chen et al., 2008; Zhai and Dai, 2009). It covers most of the area
119 within the 50 m isobaths. Domain II is off the Zhejiang-Fujian coast and featured by
120 turbid coastal waters and the Changjiang plume in winter. It has a strong seasonal
121 variation in $p\text{CO}_2$. Domains III (28.5-33.0 °N, 126.0-128.0 °E, $96 \times 10^3 \text{ km}^2$), IV
122 (27.0-28.5 °N, 123.5-128.0 °E, $65 \times 10^3 \text{ km}^2$) and V (25.0-27.0 °N, 120.0-125.4 °E,
123 $60 \times 10^3 \text{ km}^2$) are all located in the mid- and outer shelf, influenced by the Kuroshio
124 and thus characterized by lower nutrients and warm temperature. Domain III is
125 located in the northern ECS shelf and generally dominated by temperature and
126 impacted by the far field Changjiang plume in flood seasons. Domain IV is located in
127 the middle ECS shelf, characterized by low Chl-*a* all year round and high $p\text{CO}_2$ in
128 warm seasons, but is not impacted by the river plume (Bai et al., 2014). Domain V is
129 on the southern ECS shelf where $p\text{CO}_2$ is dominated by temperature and might be
130 under the influence of the northern Taiwan upwelling.

131 **3 Material and Methods**

132 **3.1 Measurements of $p\text{CO}_2$, SST, SSS and auxiliary data**

133 24 cruises/legs were conducted from 2006 to 2011 in the ECS on board R/Vs
134 *Dongfanghong II* and *Kexue III* or a fishing boat *Hubaoyu 2362*. Survey periods and
135 areas are listed in Table 2. Sampling tracks are shown in Fig. 2. During the cruises,
136 sea surface salinity (SSS), SST and $p\text{CO}_2$ were measured continuously. The methods
137 of measurement and data processing followed those of Pierrot et al. (2009) and the
138 SOCAT (Surface Ocean CO_2 Atlas, <http://www.socat.info/news.html>) protocol, which
139 are briefly summarized here.

140 $p\text{CO}_2$ was continuously measured with a non-dispersive infrared spectrometer
141 (Li-Cor® 7000) integrated in a GO-8050 underway system (General Oceanic Inc.
142 USA) on board *Dongfanghong II* or with a home-made underway system on board
143 *Kexue III* or *Hubaoyu 2362*. The GO-8050 underway system is described by Pierrot et

144 al. (2009). The home-made underway system is described by Zhai et al. (2007) and
145 Zhai and Dai (2009), with which a Jiang et al. (2008) equilibrator was employed.
146 Surface water was continuously pumped from 1.5 to 5 m depth and determined every
147 80 seconds. CO₂ concentration in the atmosphere was determined every ~ 1.5 hours.
148 The bow intake for air sampling was installed ~ 10 m above the sea surface to avoid
149 contamination from the ship. The barometric pressure was measured continuously
150 aboard with a barometer attached to a level of ~ 10 m above the sea surface. The
151 accuracy of the *p*CO₂ measurements was ~ 0.3% (Zhai and Dai, 2009).

152 **3.2 Data processing**

153 Water *p*CO₂ at the temperature in the equilibrator (*p*CO₂^{Eq}) was calculated from the
154 CO₂ concentration in the equilibrator (*x*CO₂) and the pressure in the equilibrator (*P*_{Eq})
155 after correction for the vapor pressure (*P*_{H₂O}) of water at 100% relative humidity
156 (Weiss and Price, 1980):

$$157 \quad p\text{CO}_2^{\text{Eq}} = (P_{\text{Eq}} - P_{\text{H}_2\text{O}}) \times x\text{CO}_2 \quad (1)$$

158 *p*CO₂ in the air was calculated similarly using *x*CO₂ in the air and the barometric
159 pressure. *x*CO₂ in the atmosphere over the Tae-ahn Peninsula (36.7376 °N,
160 126.1328 °E, Republic of Korea, <http://www.esrl.noaa.gov/gmd/dv/site>) was adopted
161 in the atmospheric *p*CO₂ calculation after comparison with the field measured values
162 during the surveys.

163 Water *p*CO₂^{Eq} obtained from Formula (1) was corrected to *p*CO₂ at *in situ* temperature
164 (*in situ p*CO₂, or *p*CO₂ hereafter) using the empirical formula of Takahashi et al.
165 (1993), where *t* is the temperature in the equilibrator.

$$166 \quad \textit{In situ pCO}_2 = p\text{CO}_2^{\text{Eq}} \times \exp((\text{SST} - t) \times 0.0423) \quad (2)$$

167 Net CO₂ flux (*F*_{CO₂}) between the surface water and the atmosphere (or air-sea CO₂
168 flux) was calculated using the following formula:

169 $F_{\text{CO}_2} = k \times s \times \Delta p\text{CO}_2$ (3)

170 where s is the solubility of CO_2 (Weiss, 1974); $\Delta p\text{CO}_2$ is the $p\text{CO}_2$ difference between
 171 the surface water and the atmosphere; and k is the CO_2 transfer velocity. k was
 172 parameterized using the empirical function of Sweeney et al. (2007) and nonlinear
 173 correction of gas transfer velocity with wind speed was adopted following
 174 Wanninkhof et al. (2002) and Jiang et al. (2008):

175 $k(\text{S07}) = 0.27 \times C_2 \times U_{\text{mean}}^2 \times (\text{Sc}/660)^{-0.5}$ (4)

176 $C_2 = \left(\frac{1}{n} \sum_{j=1}^n U_j^2 \right) / U_{\text{mean}}^2$ (5)

177 where U_{mean} is the monthly mean wind speed at 10 m above the sea level (in m s^{-1});
 178 and Sc is the Schmidt number at *in situ* temperature for surface seawater (Wanninkhof,
 179 1992). C_2 is the nonlinear coefficient for the quadratic term of the gas transfer
 180 relationship; U_j is the high-frequency wind speed (in m s^{-1}); the subscript "mean" is to
 181 calculate the average; and n is the number of available wind speeds in the month.
 182 Wind speeds at a spatial resolution of $1^\circ \times 1^\circ$ and temporal resolution of 6 h were
 183 obtained from the National Centers for Environmental Prediction of the United States
 184 (NCEP, <http://oceandata.sci.gsfc.nasa.gov/Ancillary/Meteorological>) and the monthly
 185 average was adopted in the CO_2 flux calculations. As defined here, a positive flux
 186 indicates an evasion of CO_2 from the sea to the air.

187 The seasonal amplitude and spatial variation in SST in the ECS are large, up to
 188 $>10^\circ \text{C}$, which significantly impacts the $p\text{CO}_2$. To distinguish the influence of
 189 biogeochemical processes from the thermodynamics effect, $p\text{CO}_2$ was normalized to a
 190 constant temperature following Takahashi et al. (2002), termed as $Np\text{CO}_2$:

191 $Np\text{CO}_2 = p\text{CO}_2 \times \exp(0.0423 \times (21 - \text{SST}))$ (6)

192 Here, 21°C was used since it corresponded to the average SST during the cruises.

193 Our surveys covered the four seasons of the year, among which we defined March to
194 May as spring, June to August as summer, September to November as fall and
195 December to February as winter.

196 At the global scale, both the atmospheric $p\text{CO}_2$ and the surface seawater $p\text{CO}_2$ are
197 increasing and the rate of increase differs in different regions (Takahashi et al., 2009).
198 Tseng et al. (2014) report that the increasing rate of $p\text{CO}_2$ is 1.9 and 2.1 $\mu\text{atm yr}^{-1}$ for
199 the atmosphere and the surface seawater, respectively, in the ECS based on the
200 observations from 1998 to 2012. We assumed that these yearly change rates were
201 evenly distributed to each month, based on which we corrected the $p\text{CO}_2$ data to June
202 2010.

203 **4 Results**

204 **4.1 SST and SSS**

205 Fig. 3 reveals strong temporal and spatial variations in SST over the 12 months of the
206 year. The seasonal variation in the average SST and SSS in the five domains is further
207 shown in Fig. 4 and Tables 3 to 7. In winter and spring, SST increased offshore and
208 from north to south with a range of ~ 8 to 25 $^{\circ}\text{C}$, and the highest SST appeared in the
209 southeastern part of the ECS. In summer and fall, SST was high and relatively
210 spatially homogeneous compared to that in winter and spring with a range of ~ 18 to
211 30 $^{\circ}\text{C}$. On a monthly time scale, the lowest SST appeared in January to March and the
212 highest in July to September (Fig. 3). The magnitude of seasonal variation in SST
213 decreased offshore, from 12 to 14 $^{\circ}\text{C}$ in Domains I and II to 6 to 8 $^{\circ}\text{C}$ in Domains IV
214 and V. The lowest SST was observed in Domain I in January 2009, which was
215 8.1 ± 0.8 $^{\circ}\text{C}$ (Fig. 4). In July and August, there was a northeastern oriented filament
216 with relatively low SST off eastern Taiwan (Fig. 3). The average SST measured
217 underway during the surveys in the entire study area was 17.8 ± 2.2 $^{\circ}\text{C}$ in winter,
218 19.7 ± 2.9 $^{\circ}\text{C}$ in spring, 26.2 ± 1.8 $^{\circ}\text{C}$ in summer and 23.2 ± 1.2 $^{\circ}\text{C}$ in fall.

219 Spatially, salinity increased offshore and the highest salinity appeared in the area

220 affected by the Kuroshio (not shown). At the whole shelf scale, the lowest salinity was
221 observed in Domain I, where it was lower in March to August (29 to 32) and higher in
222 September to February (30 to 34). The low SSS in spring and summer corresponded
223 to the high freshwater discharge of the year from the Changjiang. SSS in June was
224 relatively high compared to that in March, April, May, July and August (Fig. 4B),
225 which might be attributed to the fact that there was only one June survey (June 2011)
226 and this survey followed an exceptionally dry May. The discharge of the Changjiang
227 in May of 2011 was ~ 40% lower than the monthly average of 2005 to 2011 (data at
228 Datong gauge station, the *Hydrological Information Annual Report 2005 to 2011*,
229 Ministry of Water Resources, P. R. China). On a seasonal scale, the average SSS in
230 Domain I was lowest in spring (30.6 ± 4.6) and summer (30.9 ± 1.4) and highest in fall
231 (33.4 ± 0.9). SSS in winter (31.5 ± 2.3) was higher than in spring-summer but lower
232 than in fall. The seasonality of SSS in Domain II was different from that of Domain I
233 (Table 3), and was lower in November to February (29.6 to 34.3) than in March to
234 October (32.6 to 34.0, Fig. 4B). This seasonality might be attributed to the fact that
235 the Changjiang plume and coastal current were southwestward in winter (Han et al.,
236 2013; Lee and Chao, 2003). The seasonal variation of SSS in Domains I and II was up
237 to 2.7 to 2.8.

238 Data in Domain III were rather limited, based on which, SSS in winter (34.4 ± 0.2) and
239 fall (34.2 ± 0.1) was higher than that in summer (33.1 ± 0.6) (Table 5). The seasonality
240 of SSS in Domains IV and V was similar, showing low SSS in July to September (33
241 to 34) but high in other months (>34). Seasonal variation in SSS in these two domains
242 was <1 , which was much smaller than that in Domains I, II and III. The average
243 salinity in the entire study area was 33.2 ± 2.5 in winter, 33.3 ± 4.7 in spring, 33.0 ± 1.6 in
244 summer and 33.8 ± 1.3 in fall.

245 **4.2 Wind speeds and C_2**

246 The temporal patterns of the wind speeds in the five domains were similar (Tables 3
247 to 7). The monthly average wind speeds ranged from 5.3 to 11.4 m s^{-1} and their

248 standard deviations (SDs) were lower than 1 m s^{-1} . Generally, wind speed was high in
249 fall and winter but low in spring and summer with large inter-annual variations. The
250 highest wind speeds were recorded in Domains II, IV and V in November 2007, when
251 the monthly average wind speeds reached 10.4 to 11.4 m s^{-1} . The lowest wind speeds
252 were observed in August 2008, May 2009 and May 2011, when the monthly average
253 wind speeds ranged from 5.6 to 6.5 m s^{-1} . Wind speeds in September, October and
254 November 2006 were relatively low compared to other fall months and, in March
255 2009, were relatively high compared to other spring months.

256 C_2 ranged from 1.06 to 1.70 and the annual average C_2 in the five domains was
257 1.21 ± 0.04 , 1.20 ± 0.09 , 1.21 ± 0.06 , 1.19 ± 0.08 and 1.19 ± 0.13 , which was similar to or
258 slightly lower than the global average of 1.27 (Wanninkhof et al., 2009).

259 **4.3 CO₂ concentration in the air**

260 Field observed CO₂ concentrations in the air over the ECS ranged 370 to $410 \text{ } \mu\text{atm}$,
261 which was not inconsistent with the global increase in atmospheric $p\text{CO}_2$. Both the
262 seasonal and inter annual patterns we measured during the surveys were similar to
263 those observed at the Tae-ahn Peninsula (Korea-China Center for Atmospheric
264 Research, Republic of Korea) with the highest values typically observed in February
265 to April and the lowest values in July to September (Fig. 5). The difference in
266 atmospheric CO₂ between our ship-board measurements over the ECS and that
267 observed at the Tae-ahn Peninsula was not significant, ranging from 0.1 to 7.9 ppm
268 (average $\sim 3.5 \text{ ppm}$). However, the amplitude of the seasonal variation in air CO₂
269 concentration over the ECS was larger than that over the open North Pacific (Mauna
270 Loa station), the latter of which was 5 to 10 ppm . Both the air CO₂ concentration over
271 the ECS and the Tae-ahn Peninsula were higher than that at the Mauna Loa station,
272 which might be due to the fact that the marine boundary atmosphere over marginal
273 seas has more impacts from terrestrial sources.

274 **4.4 Surface seawater $p\text{CO}_2$**

275 $p\text{CO}_2$ values along the cruise tracks in this study are shown in Fig. 2. By averaging
276 the $p\text{CO}_2$ values on these tracks to $1^\circ \times 1^\circ$ grids, we obtained the mean $p\text{CO}_2$ values in
277 the five domains (Tables 3 to 7).

278 For the entire ECS shelf, $p\text{CO}_2$ was relatively homogeneous in winter but strong
279 spatial variations occurred in other seasons (Fig. 2). In Domain I, $p\text{CO}_2$ was generally
280 low ($<360 \mu\text{atm}$) in winter, spring and summer except in the area off the Changjiang
281 estuary mouth and in Hangzhou Bay and the northwestern corner which may be
282 influenced by the southern Yellow Sea through the Yellow Sea Coastal Current (Su,
283 1998) that carried higher CO_2 water southward. However, in fall, $p\text{CO}_2$ was generally
284 high ($>380 \mu\text{atm}$) except in October 2006. In Domain II, both the seasonal evolution
285 and the $p\text{CO}_2$ values were generally overall similar to those of Domain I, but $p\text{CO}_2$ in
286 summer was higher than in Domain I based on the limited data (Fig. 2). In Domains I
287 and II, the seasonal average $p\text{CO}_2$ values were 348 and 349 μatm in winter, 309 and
288 313 μatm in spring, 317 and 357 μatm in summer, and 393 and 388 μatm in fall
289 (Tables 3 and 4). The seasonal pattern in Domains IV and V was different showing
290 relatively low $p\text{CO}_2$ ($<360 \mu\text{atm}$) in winter, spring and fall but high ($>370 \mu\text{atm}$) in
291 summer (Fig. 2). The seasonal average $p\text{CO}_2$ values in these two domains were 341
292 and 344 μatm in winter, 318 and 345 μatm in spring, 380 and 381 μatm in summer
293 and 336 and 348 μatm in fall (Tables 6 and 7). Temporal coverage was sparse in
294 Domain III. Based on the limited data, the seasonality of $p\text{CO}_2$ in Domain III was
295 similar to those of Domains IV and V (Table 5). The seasonal variation was largest in
296 Domains I, II and III (~ 80 to $90 \mu\text{atm}$) and smallest in Domain V ($37 \mu\text{atm}$).

297 In addition to the strong seasonal variation, intra-seasonal variability was also
298 substantial. In Domain I, the intra-seasonal variation in $p\text{CO}_2$ was ~ 30 to $73 \mu\text{atm}$
299 during the winter, spring and summer cruises, but relatively smaller in fall ($<10 \mu\text{atm}$
300 excluding the October 2006 and December 2010 surveys, Table 3). In Domain II, it
301 was much smaller in winter ($<10 \mu\text{atm}$) than in other seasons (30 to $80 \mu\text{atm}$, Table 4).

302 In Domains IV and V, it was $\sim 10 \mu\text{atm}$ in winter, but relatively higher variability
303 occurred in spring and summer (14 to $55 \mu\text{atm}$, Tables 6 and 7).

304 Based on the seasonal average as shown in Fig. 6, the overall characteristics of the
305 $p\text{CO}_2$ distribution were conspicuous. In winter, the $p\text{CO}_2$ was relatively homogeneous
306 and the average $p\text{CO}_2$ in each domain ranged from 340 to $349 \mu\text{atm}$. In spring, the
307 gridded $p\text{CO}_2$ values were lower than those in winter except in the northwest corner
308 and the area near the Changjiang estuary. The seasonal average $p\text{CO}_2$ values in the
309 domains were generally lower than in winter (309 ± 60 , 313 ± 24 , 290 ± 10 , 318 ± 17 and
310 $345 \pm 12 \mu\text{atm}$ in the five domains respectively) since the high $p\text{CO}_2$ values were
311 located in very limited grids. In summer, $p\text{CO}_2$ was lower in the inner shelf and higher
312 in the outer shelf with extremely high $p\text{CO}_2$ in the northwest corner and off the
313 Changjiang estuary mouth and Hangzhou Bay. The seasonal average $p\text{CO}_2$ was
314 317 ± 72 , 357 ± 22 , 341 ± 18 , 380 ± 9.0 and $381 \pm 16 \mu\text{atm}$ in the five domains. In fall, the
315 average $p\text{CO}_2$ was $393 \pm 40 \mu\text{atm}$ in Domain I, which was significantly higher than in
316 the offshore domains (336 to $367 \mu\text{atm}$).

317 It is worth noting that the two cruises conducted in October 2006 and December 2010
318 appeared to be atypical. The results in these two cruises were significantly different
319 from other surveys in the respective seasons. In the October 2006 cruise, the $p\text{CO}_2$
320 went down to $364 \mu\text{atm}$ in Domain I and $308 \mu\text{atm}$ in Domain II, which was 29 and
321 $80 \mu\text{atm}$ lower than the averages of other fall cruises in the two domains. In the
322 December 2010 cruise, $p\text{CO}_2$ in Domain I was up to $384 \mu\text{atm}$, which was $36 \mu\text{atm}$
323 higher than the average $p\text{CO}_2$ of the other winter cruises (Fig. 6). We will further
324 discuss these cruises in the *Discussion* section.

325 The distribution of the SD of $p\text{CO}_2$ showed strong spatial and seasonal variations with
326 a large range of 1 to $185 \mu\text{atm}$ (Fig. 6). In Domain I, the SD was low in winter and
327 high in spring and summer. The highest SD occurred in summer in the coastal area off
328 the Changjiang estuary mouth and in Hangzhou Bay with the highest value of 80 to
329 $185 \mu\text{atm}$. The SD in Domain II ranged from 1 to $48 \mu\text{atm}$ with higher values in

330 spring and summer. In Domain III, the range of SD was 1 to 19 μatm and showed no
331 remarkable seasonal pattern. In Domains IV and V, the SD range was 1 to 29 μatm
332 with relatively higher values in spring and fall but lower in winter and summer in
333 Domain IV, and higher in spring and summer but lower in fall and winter in Domain V.
334 Since $p\text{CO}_2$ distribution was generally homogeneous in winter except in December
335 2010, as expected, the SD in winter was relatively low and in >85% grids was <10
336 μatm and the highest SD was 17 μatm . The SD in October 2006 in Domain I was
337 higher than the other fall surveys and the SD in Domain I in December 2010 was
338 higher than the other winter surveys.

339 It should be noted that the SD of $p\text{CO}_2$ represents the mixture of sources of
340 uncertainty in the gridded $p\text{CO}_2$ data, the analytical error, the spatial variance, and the
341 bias from undersampling. Wang et al. (2014) demonstrate that the analytical errors are
342 almost the same on the ECS shelf and the latitudinal distribution of SD is similar to
343 that of the spatial variance. Thus, higher SD usually reflects higher spatial variance
344 and vice versa along latitudes. However, the SD was equivalent to neither the spatial
345 variance nor the bulk uncertainty and the bias from undersampling may exert the
346 greatest uncertainty on the gridded $p\text{CO}_2$ in grids with poor sampling coverage (Wang
347 et al., 2014).

348 **4.5 Air-sea CO_2 fluxes**

349 Similar to the different seasonality of $p\text{CO}_2$ in the differing domains, the air-sea CO_2
350 fluxes also had strong seasonal variations in each domain and the seasonal pattern
351 differed among the domains (Tables 3 to 7).

352 Domain I was a sink of atmospheric CO_2 during all the winter, spring and summer
353 surveys with CO_2 fluxes ranging from -14.0 to -1.6 $\text{mmol m}^{-2} \text{d}^{-1}$. However, Domain I
354 in fall was a weak source of $2.2 \pm 6.8 \text{ mmol m}^{-2} \text{d}^{-1}$, with a flux range of 1.9 to 2.7
355 $\text{mmol m}^{-2} \text{d}^{-1}$ (Table 3). The CO_2 fluxes we estimated were similar to those estimated
356 by Zhai and Dai (2009) based on multiple observations (-10.4 ± 2.3 , -8.8 ± 5.8 , $-4.9 \pm$

357 4.0 and 2.9 ± 2.9 mmol m⁻² d⁻¹ in winter, spring, summer and fall, respectively).

358 Similar to Domain I, Domain II was also a strong sink in winter and spring with a
359 CO₂ flux range of -15.7 to -7.5 mmol m⁻² d⁻¹. The seasonal average flux was -8.9 ± 1.4
360 mmol m⁻² d⁻¹ in winter and -10.7 ± 3.5 mmol m⁻² d⁻¹ in spring. The sink weakened in
361 summer and the seasonal average CO₂ flux was -2.4 ± 3.3 mmol m⁻² d⁻¹. In fall,
362 Domain II was a CO₂ source of 0.7 ± 4.1 mmol m⁻² d⁻¹ (Table 4).

363 Although considerable variability occurred, Domains III, IV and V were generally
364 strong sinks in winter, spring and fall (-3.7 to -18.7 mmol m⁻² d⁻¹) but weak to
365 moderate sources in summer (0 to 6.8 mmol m⁻² d⁻¹ except in June 2011 when it was a
366 strong sink). On a seasonal time scale, CO₂ fluxes in Domains III, IV and V ranged
367 from -10.0 to -10.8 mmol m⁻² d⁻¹ in winter, -6.8 to -17.8 mmol m⁻² d⁻¹ in spring; -3.7
368 to -9.3 mmol m⁻² d⁻¹ in fall; and 1.0 to 1.8 mmol m⁻² d⁻¹ in summer (Tables 5, 6 and
369 7).

370 The annual mean CO₂ fluxes were -6.2 ± 9.1 mmol m⁻² d⁻¹ in Domain I, -5.3 ± 3.7 mmol
371 m⁻² d⁻¹ in Domain II, -9.2 ± 4.2 mmol m⁻² d⁻¹ in Domain III, -7.5 ± 1.7 mmol m⁻² d⁻¹ in
372 Domain IV and -5.9 ± 3.4 mmol m⁻² d⁻¹ in Domain V (Fig. 7). The area-weighted
373 annual mean CO₂ flux was $-6.9 \pm (4.0)$ mmol m⁻² d⁻¹ (Fig. 7), which was more than
374 twice the global average of ocean margins (Chen et al., 2013; Dai et al., 2013). Based
375 on these CO₂ fluxes, the five domains absorbed $4.9 (\pm 4.4)$, $0.9 (\pm 0.4)$, $3.8 (\pm 1.0)$,
376 $2.1 (\pm 0.3)$ and $1.5 (\pm 0.5) \times 10^{12}$ g C yr⁻¹, and the ECS shelf $13.2 (\pm 4.6) \times 10^{12}$ g C yr⁻¹ of
377 atmospheric CO₂.

378 **5 Discussion**

379 **5.1 Major controls of surface water pCO₂**

380 Because of the significant zonal difference in seasonality shown in both pCO₂ and
381 CO₂ fluxes, we discuss the major controls of pCO₂ in the five domains categorized.
382 This discussion is primarily based on the relationships of the *in situ* and normalized

383 $p\text{CO}_2$ ($Np\text{CO}_2$, normalized to 21 °C in this study) with the other parameters in each
384 domain. Since the Changjiang plume and coastal regions are strongly influenced by
385 biological activities and/or the terrestrial high- $p\text{CO}_2$ waters (Tseng et al., 2014; Zhai
386 and Dai, 2009), we used the data collected from the offshore area (Domains IV and V)
387 to obtain the "background" $Np\text{CO}_2$. In these two domains, $Np\text{CO}_2$ ranged from 250 to
388 400 μatm , and so we used $250 \times \exp((\text{SST}-21) \times 0.0423)$ and $400 \times$
389 $\exp((\text{SST}-21) \times 0.0423)$ μatm as the lower and upper limits of thermodynamically
390 dominated $p\text{CO}_2$ on the entire ECS shelf.

391 In Domains I and II, $p\text{CO}_2$ showed no conspicuous trend with SST on the yearly time
392 scale (Fig. 8). However, within individual seasons, the temperature effect on $p\text{CO}_2$
393 can be revealed. In winter, most data were above the upper limit of the
394 thermodynamically dominated $p\text{CO}_2$, suggesting extra CO_2 added to the surface water.
395 In summer, many data were below the lower limit of the thermodynamically
396 dominated $p\text{CO}_2$, indicating biogeochemical uptake of CO_2 . The $p\text{CO}_2$ in these two
397 domains neither showed clear trends with salinity, but in winter, it generally decreased
398 with SSS (Fig. 9). It is thus suggested that other processes in addition to SST and
399 estuarine mixing also played important roles in the $p\text{CO}_2$ variability, including aerobic
400 respiration, biological productivity, terrestrial input and ventilation, amongst other
401 factors.

402 The Changjiang river and estuarine water were characterized by high $p\text{CO}_2$ resulting
403 mainly from aerobic respiration (Zhai et al., 2007). In Domain I, the area off the
404 Changjiang estuary and the coastal area were influenced by the high- $p\text{CO}_2$ estuarine
405 water (Fig. 2). On the other hand, in warm seasons, the plume water was stratified and
406 biological productivity lowered the surface water $p\text{CO}_2$ as indicated by the high Chl-*a*
407 concentration in spring and summer (Fig. 10). $Np\text{CO}_2$ generally decreased with the
408 increase in Chl-*a* concentration. Although $p\text{CO}_2$ showed no relationship with SST or
409 SSS, $Np\text{CO}_2$ showed a decreasing pattern with SST and the lowest $Np\text{CO}_2$ occurred
410 in the warm seasons, which was consistent with the highest productivity (Figs 8 and

411 10). In fall, vertical stratification collapsed and the CO₂-enriched subsurface and
412 bottom waters mixed into the surface and increased the surface water *p*CO₂. In winter
413 and early fall, the cooling effect decreased *p*CO₂ and resulted in Domain I acting as a
414 CO₂ sink in the cold seasons. If the *p*CO₂ in winter was taken as the reference, the
415 calculated thermodynamically controlled *p*CO₂ in spring would be 379.3 μatm. The
416 observed *p*CO₂ in spring was 70.4 μatm lower than the thermodynamically mediated
417 *p*CO₂. Similarly, if spring was taken as a reference, the thermodynamically mediated
418 *p*CO₂ in summer would be 479.0 μatm and the observed *p*CO₂ was 161.8 μatm lower
419 than this value. These differences might be the CO₂ drawdown mainly mediated by
420 biological activities. Similarly, the observed *p*CO₂ was 100.5 μatm higher than the
421 thermodynamically mediated *p*CO₂ (293.0 μatm) in fall, which might be due mainly
422 to the mixing of the CO₂-rich subsurface/bottom water in fall, when vertical mixing
423 was enhanced. It should be noted that the CO₂ system is a buffer system and the *p*CO₂
424 response is much slower (Zhai et al., 2014). Therefore the above estimation is to
425 explain the biological effect on *p*CO₂ qualitatively rather than to make an accurate
426 calculation.

427 Controls of *p*CO₂ in Domain II were similar to but more complex than those in
428 Domain I. Cooling and biological uptake were responsible for the strong sink in
429 winter and spring. However, in summer biological uptake of CO₂ was limited since it
430 was beyond the productive area (Fig. 10), so the CO₂ flux was controlled by both
431 biological activities and heating effect. In fall, cooling was important in drawing
432 down *p*CO₂ and the influence of vertical mixing was not significant since the hypoxia
433 and thus the high-*p*CO₂ bottom water was limited to Domain I (Chen et al., 2007;
434 Wang et al., 2012).

435 In Domains IV and V, *p*CO₂ in summer was higher than that in the other seasons (Fig.
436 2). The *p*CO₂ generally increased with SST but showed no trend with SSS (Figs 8 and
437 9). This suggests that temperature was an important factor influencing *p*CO₂. Neither
438 *p*CO₂ nor *Np*CO₂ showed conspicuous trends with Chl-*a* concentration, and Chl-*a*

439 concentration was relatively low ($<2 \mu\text{g L}^{-1}$, Fig. 10). This suggests that, for a
440 particular season, productivity was not the dominating process in the spatial
441 distribution of $p\text{CO}_2$. Comparison among the seasons showed that the $Np\text{CO}_2$ was
442 highest in winter and lowest in summer. This might be due to the weak mixing of the
443 CO_2 -rich subsurface water in summer. Additionally, the lowest $Np\text{CO}_2$ values in
444 summer might suggest that the potential biological uptake of CO_2 was strong in
445 summer, although biological uptake was not a dominating factor. Although $Np\text{CO}_2$
446 was lowest in summer, *in situ* $p\text{CO}_2$ was highest, indicating that high temperature
447 increased $p\text{CO}_2$ in the warm seasons. With similar calculations conducted in Domain I,
448 the estimated $p\text{CO}_2$ drawdown would be 25 to 39 μatm in spring and summer and the
449 $p\text{CO}_2$ increase in fall would range from 21 to 35 μatm due to enhanced vertical
450 mixing. These values were much lower than the dynamic inshore areas (Domains I
451 and II) and might be negligible and the re-equilibrium of CO_2 takes a longer time than
452 the 3 month long seasons defined here (Zhai et al., 2014). The major controls of $p\text{CO}_2$
453 in Domain III were between those of Domains I/II and IV/V.

454 In summary, the ECS shelf is heterogeneous in both CO_2 fluxes and their controls.
455 The $p\text{CO}_2$ of the inner shelf waters (Domains I and II) was mainly dominated by the
456 biological uptake of CO_2 in spring/summer and cooling in winter, which induced the
457 moderate to strong sink in the three seasons, while in fall mixing with CO_2 -rich
458 bottom/subsurface water was attributed to the CO_2 release. However, the offshore
459 areas (Domains IV and V) were dominated mainly by temperature.

460 The CO_2 sink is dominated by the high biological productivity in summer (Chou et al.,
461 2009), which appears to have close correlation with the Changjiang riverine discharge
462 (Tseng et al., 2011; Tseng et al., 2014). However, cooling is attributed to be the major
463 driver of the CO_2 sink in winter (Tsunogai et al., 1999). In the northern ECS and in
464 the area off the Changjiang estuary, vertical mixing of the CO_2 -rich subsurface/bottom
465 waters is attributed to the CO_2 source in fall (Kim et al., 2013; Zhai and Dai, 2009).
466 Shim et al. (2007) suggest that $p\text{CO}_2$ in the northeastern ECS is dominated by

467 temperature but in the northwestern ECS, the main controlling factor is more
468 seasonally complex. Based on the data collected from single cruise in summer, fall
469 and winter, Chou et al. (2013) suggest that $p\text{CO}_2$ is dominated by biological
470 production on the inner shelf and by temperature on the outer shelf.

471 Based on the data collected mainly in the inner and middle ECS shelves and limited
472 field surveys in cold seasons, Tseng et al. (2014) suggest that the Changjiang
473 discharge is the primary factor that governs the CO_2 sink for the entire ECS. The
474 dataset covering complete seasonal and spatial coverage presented in this study
475 suggested that zonal assessment is important to obtain a comprehensive picture of
476 CO_2 flux and its control in the dynamic marginal seas. Extrapolation from the data
477 collected in the river-dominated area to the entire ECS shelf could be misleading.

478 **5.2 Intra-seasonal variation in CO_2 fluxes**

479 With the five domains categorized, we have seen overall well defined seasonality in
480 both $p\text{CO}_2$ and CO_2 fluxes in the individual domains, and significant intra-seasonal
481 changes occurred, which could affect the overall carbon budgeting on a longer
482 seasonal and/or annual time scale.

483 The intra-seasonal variation in the CO_2 fluxes was generally low in winter (typically
484 <2 fold variations), but it was very high in summer (4 to 6 fold) and spring (2 to 3
485 fold). Spatially, the largest intra-seasonal variability was in Domain I. The
486 intra-seasonal variation in the calculated CO_2 flux in this study was attributed to the
487 intra-seasonal variability in $\Delta p\text{CO}_2$, wind speeds, and C_2 . In the five domains, the
488 highest value of C_2 was 1.1 to 1.4 fold of the lowest value within each season, which
489 did not induce remarkable intra-seasonal variability in the calculated CO_2 flux.
490 However, intra-seasonal variability in wind speed and $\Delta p\text{CO}_2$ might have induced
491 large variability in the calculated CO_2 fluxes. The highest wind speed was 1.1 to 1.2
492 fold the lowest value in winter and 1.2 to 1.6 fold those in spring, summer and fall in
493 each domain. This might have caused 1.2 to 1.4 fold variation in winter and 1.4 to 2.6

494 fold variation in other seasons in the calculated CO₂ fluxes. The intra-seasonal
495 variability in wind speed showed no spatial pattern. The intra-seasonal variation in
496 $\Delta p\text{CO}_2$ was generally high in summer and spring but low in winter and fall. The
497 largest intra-seasonal variation was observed in Domain I in summer and spring. In
498 summer, the lowest $\Delta p\text{CO}_2$ was -85 μatm in June 2006, which was 6.9 fold that in
499 July 2009 (-12 μatm). The intra-seasonal variation in $\Delta p\text{CO}_2$ in spring was smaller
500 than in summer but still very large (3.5 fold).

501 Additionally, atypical surveys increased the intra-seasonal variations. One example
502 was the October 2006 cruise. Under typical fall conditions, Domain I is a source of
503 atmospheric CO₂ when stratification starts to weaken and strong vertical mixing starts
504 leading to the release of subsurface CO₂ (Zhai and Dai, 2009). In October 2006,
505 however, average $p\text{CO}_2$ was down to 364 μatm in Domain I, which was 29 μatm
506 lower than the seasonal average based on the data collected during all the other
507 surveys in fall (394 μatm) (Table 3). The low $p\text{CO}_2$ in Oct 2006 might be induced by
508 a local bloom as reflected by the high degree of oxygen saturation in the surface water.
509 Dissolved oxygen increased to 120% to 130% in a local area off Hangzhou Bay and
510 the Changjiang estuary, which was a significant increase from September 2006 when
511 the degree of oxygen saturation ranged from 90 to 110% (Fig. A1 in the Appendix).
512 This local bloom caused Domain I to act as a CO₂ sink of 1.9 $\text{mmol m}^{-2} \text{d}^{-1}$ as
513 compared to a CO₂ source of 2.2 $\text{mmol m}^{-2} \text{d}^{-1}$ based on the data collected from all the
514 other fall surveys (Table 3). If this survey was included into the flux estimation, the
515 seasonal average CO₂ flux in fall would be 1.2 ± 6.4 in Domain I. This CO₂ source
516 strength was ~ 54% of the average of the other fall cruises in Domain I. However,
517 inclusion of the October 2006 survey into the fall cruises would result in an annual
518 CO₂ flux of $-7.1 \pm 3.9 \text{ mmol m}^{-2} \text{d}^{-1}$, which is not significantly different from the
519 estimate of $-6.9 \pm 4.0 \text{ mmol m}^{-2} \text{d}^{-1}$ excluding the October 2006 cruise. This was
520 because we had multiple cruise observations in fall and the fall bloom was only
521 observed in a very small area of the ECS.

522 In the temperate seas, blooms occur in both spring and fall, which are mainly
523 controlled by light availability and nutrient supply (Lalli and Parsons, 1993; Martinez
524 et al., 2011). In the ECS, there is no report on fall blooms in the near shore area. The
525 occurrence of a fall bloom and its influence on the CO₂ flux needs further study.

526 Another example is the early winter cruise (based on our seasonal category) in 2010
527 which was conducted on 1-11 December. The average SST was 5.5 °C higher than the
528 average SST during other winter surveys in Domain I. Also, the pCO₂ distribution
529 pattern was similar to that in fall. As a result, Domain I was a weak sink of -1.6 mmol
530 m⁻² d⁻¹ during this early December cruise, which was only 16% of the average CO₂
531 sink based on the data collected during the other winter cruises (-9.8 mmol m⁻² d⁻¹).
532 We concluded that this early December 2010 survey was conducted during the
533 transitional period between typical fall and winter, which would be difficult to be
534 categorized into any season. If the December 2010 survey was grouped into the fall
535 cruises, the seasonal average CO₂ flux in Domain I in fall would be 1.2±7.1 mmol m⁻²
536 d⁻¹ and the annual CO₂ flux in the entire ECS would be -7.4±4.1 mmol m⁻² d⁻¹.
537 However, if the December 2010 survey was grouped into the winter cruises, the
538 seasonal average CO₂ flux in Domain I in winter would be -8.4±5.3 mmol m⁻² d⁻¹ and
539 the annual CO₂ flux in the entire ECS would be -6.9±4.1 mmol m⁻² d⁻¹.

540 The strong CO₂ sink in the ECS might be attributed to the generally low surface water
541 pCO₂. As discussed in Section 5.1, the strong biological uptake in spring/summer and
542 strong cooling in winter were the major controls of the low pCO₂ in the ECS. Primary
543 production on the ECS shelf ranges from 0.2 to 2.0 g C m⁻² d⁻¹ in warm seasons
544 (Gong et al., 2003). During our spring and summer cruises, Chl-*a* concentration was
545 up to 20 or even 40 µg L⁻¹. Both the phytoplankton biomass and the primary
546 production are among the highest in the world marginal seas such as the Barents Sea
547 (Dalpadado et al., 2014), the Beaufort Sea (Carmack et al., 2004), the South Atlantic
548 Bight (Martins and Pelegri, 2006), and the South China Sea (Chen, 2005). In addition,
549 the ECS is located in the mid latitude zone with strong seasonality. In winter, the low

550 temperature draws surface water $p\text{CO}_2$ well below the atmospheric $p\text{CO}_2$, drawing
551 down $\sim 140 \mu\text{atm}$ with 10°C decrease from $\sim 400 \mu\text{atm}$.

552 This study reports what we believe to be a most comprehensive dataset of CO_2 fluxes
553 based on field measurements with a full coverage of the ECS shelf at a temporal
554 resolution of seasonal scale. Table 8 shows comparisons of the CO_2 fluxes estimated
555 in this study with others in the ECS. For ease of comparison, we standardized the CO_2
556 flux estimation using the Sweeney et al. (2007) gas transfer velocity algorithms. For
557 the results calculated using long-term (or monthly) average wind speeds, we
558 multiplied C_2 (~ 1.2) to make them consistent with our estimation. The CO_2 fluxes
559 calculated using the algorithm of Ho et al. (2006) were the same as those of Sweeney
560 et al. (2007).

561 Comparison between our results and the CO_2 fluxes estimated based on multiple
562 observations (such as those of Zhai and Dai 2009) were similar in Domain I in all
563 seasons (the differences were $<35\%$, Table 8). However, the CO_2 flux estimations
564 based on limited surveys in spring, the season with strong intra-seasonal variability,
565 such as those of Kim et al. (2013) and Shim et al. (2007) in Domains I and III, and
566 Peng et al. (1999) in Domains III, IV and V, were often different from our results.
567 However, the CO_2 flux based on a single survey in winter by Chou et al. (2011) on the
568 entire ECS shelf, Shim et al. (2007) and Kim et al. (2013) in Domains I and III were
569 similar to our results, which is likely due to the relatively smaller inter-seasonal
570 variability in winter. For the entire ECS, the CO_2 fluxes in spring and summer
571 estimated by Tseng et al. (2011; 2014) are similar to our estimate based on field
572 surveys. However, there is a large difference in the fall results. The good consistency
573 of the Tseng et al. (2011; 2014) results with ours in spring and summer might be due
574 to the fact that their empirical algorithm is mainly based on field data collected in
575 warmer seasons.

576 We have demonstrated that field observations with full consideration of seasonal
577 variability is necessary to constrain CO_2 fluxes with large heterogeneity in both time

578 and space. We must point out, however, that it remains difficult to fully resolve the
579 intra-seasonal changes in dynamic shelf seas, in particularly in areas such as Domains
580 I and II. High-frequency observation in the seasons and/or locations with largest
581 variability and/or with poor understanding in the mechanisms controlling $p\text{CO}_2$ are
582 clearly needed to reduce the error from undersampling and to further improve
583 estimates of CO_2 fluxes.

584 **6 Concluding remarks**

585 Surface water $p\text{CO}_2$ and air-sea CO_2 fluxes in the ECS shelf show strong temporal
586 and spatial variations, despite which, the $p\text{CO}_2$ and associated fluxes are robustly well
587 defined. The Changjiang plume is a moderate to strong CO_2 sink in spring, summer
588 and winter, but it is a weak CO_2 source in fall. The middle and southern ECS shelves
589 are a CO_2 source in summer but a strong CO_2 sink in other seasons. Major controls of
590 $p\text{CO}_2$ differ in different domains. Domains I and II were mainly dominated by
591 biological CO_2 uptake in spring and summer, ventilation in fall and cooling in winter,
592 while Domains IV and V were dominated by temperature over the whole year. On an
593 annual basis, the entire ECS shelf is a CO_2 sink of $6.9 (\pm 4.0) \text{ mmol m}^{-2} \text{ d}^{-1}$ and it
594 sequesters 13.2 Tg C from the atmosphere annually based on our observations from
595 2006 to 2011. This study suggested that zonal assessment of CO_2 fluxes and study of
596 the major controls were necessary in the dynamic marginal seas.

597 **Acknowledgements**

598 This study was jointly supported by the National Basic Research Program of China
599 through grant 2009CB421200 (the CHOICE-C project) and 2015CB954001
600 (CHOICE-C II), and Natural Science Foundation of China through grants 41076044
601 and 41121091, and the State Oceanic Administration of China through contract
602 DOMEPP-MEA-01-10. Sampling cruises were partially supported by the National
603 High-Tech Research and Development Program ("863" Program) of China (via the
604 projects of Quality Control / *in situ* Standardization Experiment 2007 and 2008) and
605 the National Basic Research Program of China (grant 2005CB422300). We are

606 grateful to the crew and scientific staff of R/V Dongfanghong II for their help during
607 these large-scale surveys. Yuancheng Su and Jinwen Liu are appreciated for the data
608 collection during some of the cruises. We acknowledge the constructive comments
609 from three anonymous reviewers, which improved the quality of our paper. Professor
610 John Hodgkiss is thanked for polishing the English in this paper.

611 **References**

- 612 Bai, Y., He, X., Pan, D., Chen, C.-T.A., Kang, Y., Chen, X. and Cai, W.-J., 2014.
613 Summertime Changjiang River plume variation during 1998–2010. *Journal of*
614 *Geophysical Research: Oceans*, 119(9): 6238-6257.
- 615 Borges, A.V., Delille, B. and Frankignoulle, M., 2005. Budgeting sinks and sources of
616 CO₂ in the coastal ocean: Diversity of ecosystems counts. *Geophysical*
617 *Research Letters*, 32(14): L14601, doi:10.1029/2005GL023053.
- 618 Cai, W.-J., Dai, M.H. and Wang, Y.-C., 2006. Air-sea exchange of carbon dioxide in
619 ocean margins: A province-based synthesis. *Geophysical Research Letters*,
620 33(12): L12603, doi:10.1029/2006GL026219.
- 621 Cai, W.J. and Dai, M., 2004. Comment on "Enhanced open ocean storage of CO₂
622 from shelf sea pumping". *Science*, 306(5701): 1477-1477.
- 623 Carmack, E.C., Macdonald, R.W. and Jasper, S., 2004. Phytoplankton productivity on
624 the Canadian Shelf of the Beaufort Sea. *Marine Ecology Progress Series*, 277:
625 37-50.
- 626 Chen, C.C., Gong, G.C. and Shiah, F.K., 2007. Hypoxia in the East China Sea: One of
627 the largest coastal low-oxygen areas in the world. *Marine Environmental*
628 *Research*, 64(4): 399-408.
- 629 Chen, C.T.A. and Borges, A.V., 2009. Reconciling opposing views on carbon cycling
630 in the coastal ocean: Continental shelves as sinks and near-shore ecosystems
631 as sources of atmospheric CO₂. *Deep-Sea Research II*, 56(8-10): 578-590.
- 632 Chen, C.T.A., Huang, T.H., Chen, Y.C., Bai, Y., He, X. and Kang, Y., 2013. Air-sea
633 exchanges of CO₂ in the world's coastal seas. *Biogeosciences*, 10(10):
634 6509-6544.

- 635 Chen, C.T.A. and Wang, S.L., 1999. Carbon, alkalinity and nutrient budgets on the
636 East China Sea continental shelf. *Journal of Geophysical Research*, 104(C9):
637 20675-20686.
- 638 Chen, C.T.A., Zhai, W. and Dai, M., 2008. Riverine input and air-sea CO₂ exchanges
639 near the Changjiang (Yangtze River) Estuary: Status quo and implication on
640 possible future changes in metabolic status. *Continental Shelf Research*,
641 28(12): 1476-1482.
- 642 Chen, Y.-L.L., 2005. Spatial and seasonal variations of nitrate-based new production
643 and primary production in the South China Sea. *Deep-Sea Research I*, 52(2):
644 319-340.
- 645 Chou, W.-C., Gong, G.-C., Cai, W.-J. and Tseng, C.-M., 2013. Seasonality of CO₂ in
646 coastal oceans altered by increasing anthropogenic nutrient delivery from large
647 rivers: evidence from the Changjiang–East China Sea system. *Biogeosciences*,
648 10: 3889-3899.
- 649 Chou, W.C., Gong, G.C., Sheu, D.D., Hung, C.C. and Tseng, T.F., 2009. Surface
650 distributions of carbon chemistry parameters in the East China Sea in summer
651 2007. *Journal of Geophysical Research*, 114(C07): C07026,
652 doi:10.1029/2008JC005128.
- 653 Chou, W.C., Gong, G.C., Tseng, C.M., Sheu, D.D., Hung, C.C., Chang, L.P. and Wang,
654 L.W., 2011. The carbonate system in the East China Sea in winter. *Marine*
655 *Chemistry*, 123(1-4): 44-55.
- 656 Chou, W.C., Sheu, D.D., Lee, B.S., Tseng, C.M., Chen, C.T.A., Wang, S.L. and Wong,
657 G.T.F., 2007. Depth distributions of alkalinity, TCO₂ and $\delta^{13}\text{C}$ (TCO₂) at
658 SEATS time-series site in the northern South China Sea. *Deep-Sea Research II*,
659 54(14-15): 1469-1485.
- 660 Dai, A. and Trenberth, K.E., 2002. Estimates of freshwater discharge from continents:
661 Latitudinal and seasonal variations. *Journal of Hydrometeorology*, 3(6):
662 660-687.
- 663 Dai, M., Cao, Z., Guo, X., Zhai, W., Liu, Z., Yin, Z., Xu, Y., Gan, J., Hu, J. and Du, C.,
664 2013. Why are some marginal seas sources of atmospheric CO₂? *Geophysical*

665 Research Letters, 40: 2154-2158.

666 Dai, M.H., Lu, Z.M., Zhai, W.D., Chen, B.S., Cao, Z.M., Zhou, K.B., Cai, W.J. and
667 Chen, C.T.A., 2009. Diurnal variations of surface seawater $p\text{CO}_2$ in
668 contrasting coastal environments. *Limnology and Oceanography*, 54(3):
669 735-745.

670 Dalpadado, P., Arrigo, K.R., Hjollo, S.S., Rey, F., Ingvaldsen, R.B., Sperfeld, E., van
671 Dijken, G.L., Stige, L.C., Olsen, A. and Ottersen, G., 2014. Productivity in the
672 Barents Sea - Response to Recent Climate Variability. *Plos One*, 9(5).

673 Gong, G.C., Wen, Y.H., Wang, B.W. and Liu, G.J., 2003. Seasonal variation of
674 chlorophyll a concentration, primary production and environmental conditions
675 in the subtropical East China Sea. *Deep-Sea Research II*, 50(6-7): 1219-1236.

676 Han, A., Dai, M., Gan, J., Kao, S., Zhao, X.Z., Jan, S., Li, Q., Lin, H., Chen, C.T.A.,
677 Wang, L., Hu, J., Wang, L. and Gong, F., 2013. Inter-shelf nutrient transport
678 from the East China Sea as a major nutrient source supporting winter primary
679 production on the northern South China Sea shelf. *Biogeosciences*, 10:
680 8159-8170.

681 He, X., Bai, Y., Pan, D., Chen, C.-T.A., Cheng, Q., Wang, D. and Gong, F., 2013.
682 Satellite views of seasonal and inter-annual variability of phytoplankton
683 blooms in the eastern China seas over the past 14 yr (1998-2011).
684 *Biogeosciences*, 10(7): 4721-4739.

685 Ho, D.T., Law, C.S., Smith, M.J., Schlosser, P., Harvey, M. and Hill, P., 2006.
686 Measurements of air-sea gas exchange at high wind speeds in the Southern
687 Ocean: Implications for global parameterizations. *Geophysical Research*
688 *Letters*, 33(16): L16611, doi:10.1029/2006GL026817.

689 Jiang, L.Q., Cai, W.J., Wanninkhof, R., Wang, Y.C. and Luger, H., 2008. Air-sea CO_2
690 fluxes on the US South Atlantic Bight: Spatial and seasonal variability. *Journal*
691 *of Geophysical Research-Oceans*, 113(C7): C07019,
692 doi:10.1029/2007JC004366.

693 Kim, D., Choi, S.-H., Shim, J.-H., Kim, K.-H. and Kim, C.-H., 2013. Revisiting the
694 seasonal variations of sea-air CO_2 fluxes in the northern East China Sea.

695 Terrestrial Atmospheric and Oceanic Sciences, 24(3): 409-419.

696 Lalli, C.M. and Parsons, T.R., 1993. Biological Oceanography: An Introduction.
697 Butterworth Heinemann, Burlington.

698 Laruelle, G.G., Durr, H.H., Slomp, C.P. and Borges, A.V., 2010. Evaluation of sinks
699 and sources of CO₂ in the global coastal ocean using a spatially-explicit
700 typology of estuaries and continental shelves. Geophysical Research Letters,
701 37(15): L15607, doi:10.1029/2010GL043691.

702 Laruelle, G.G., Lauerwald, R., Pfeil, B. and Regnier, P., 2014. Regionalized global
703 budget of the CO₂ exchange at the air-water interface in continental shelf seas.
704 Global Biogeochemical Cycles, 28(11): 1199-1214.

705 Lee, H.J. and Chao, S.Y., 2003. A climatological description of circulation in and
706 around the East China Sea. Deep-Sea Research II, 50(6-7): 1065-1084.

707 Liss, P.S. and Merlivat, L., 1986. Air-sea gas exchange rates: introduction and
708 synthesis. In: P. Buat-Menard (Editor), The Role of Air-Sea Exchange in
709 Geochemical Cycling. Reidel, Hingham, MA, pp. 113-129.

710 Liu, Z. and Gan, J., 2012. Variability of the Kuroshio in the East China Sea derived
711 from satellite altimetry data. Deep-Sea Research I, 59: 25-36.

712 Martinez, E., Antoine, D., D'Ortenzio, F. and de Boyer Montegut, C., 2011.
713 Phytoplankton spring and fall blooms in the North Atlantic in the 1980s and
714 2000s. Journal of Geophysical Research, 116(C11): C11029,
715 doi:10.1029/2010JC006836.

716 Martins, A.M. and Pelegri, J.L., 2006. CZCS chlorophyll patterns in the South
717 Atlantic Bight during low vertical stratification conditions. Continental Shelf
718 Research, 26(4): 429-457.

719 Omar, A., Johannessen, T., Kaltin, S. and Olsen, A., 2003. Anthropogenic increase of
720 oceanic pCO₂ in the Barents Sea surface water. Journal of Geophysical
721 Research, 108(C12): 3388, doi:10.1029/2002JC001628.

722 Peng, T.H., Hung, J.J., Wanninkhof, R. and Millero, F.J., 1999. Carbon budget in the
723 East China Sea in spring. Tellus B, 51(2): 531-540.

724 Pierrot, D., Neill, C., Sullivan, K., Castle, R., Wanninkhof, R., Luger, H., Johannessen,

725 T., Olsen, A., Feely, R.A. and Cosca, C.E., 2009. Recommendations for
726 autonomous underway $p\text{CO}_2$ measuring systems and data-reduction routines.
727 Deep-Sea Research II, 56(8-10): 512-522.

728 Shim, J., Kim, D., Kang, Y.C., Lee, J.H., Jang, S.T. and Kim, C.H., 2007. Seasonal
729 variations in $p\text{CO}_2$ and its controlling factors in surface seawater of the
730 northern East China Sea. Continental Shelf Research, 27(20): 2623-2636.

731 Su, J., 1998. Circulation dynamics of the China Seas north of 18 N coastal segment.
732 In: A.R. Robinson and K.H. Brink (Editors), The Sea (Vol. 11). John Wiley &
733 Sons, Inc., New York, pp. 483-505.

734 Sweeney, C., Gloor, E., Jacobson, A.R., Key, R.M., McKinley, G., Sarmiento, J.L. and
735 Wanninkhof, R., 2007. Constraining global air-sea gas exchange for CO_2 with
736 recent bomb C-14 measurements. Global Biogeochemical Cycles, 21(2):
737 GB2015, doi:10.1029/2006GB002784.

738 Takahashi, T., Olafsson, J., Goddard, J.G., Chipman, D.W. and Sutherland, S.C., 1993.
739 Seasonal variation of CO_2 and nutrients in the high latitude surface oceans-A
740 comparative study. Global Biogeochemical Cycles, 7(4): 843-878.

741 Takahashi, T., Sutherland, S.C., Sweeney, C., Poisson, A., Metzl, N., Tilbrook, B.,
742 Bates, N., Wanninkhof, R., Feely, R.A., Sabine, C., Olafsson, J. and Nojiri, Y.,
743 2002. Global sea-air CO_2 flux based on climatological surface ocean $p\text{CO}_2$,
744 and seasonal biological and temperature effects. Deep-Sea Research II,
745 49(9-10): 1601-1622.

746 Takahashi, T., Sutherland, S.C., Wanninkhof, R., Sweeney, C., Feely, R.A., Chipman,
747 D.W., Hales, B., Friederich, G., Chavez, F., Sabine, C., Watson, A., Bakker,
748 D.C.E., Schuster, U., Metzl, N., Yoshikawa-Inoue, H., Ishii, M., Midorikawa,
749 T., Nojiri, Y., Kortzinger, A., Steinhoff, T., Hoppema, M., Olafsson, J.,
750 Arnarson, T.S., Tilbrook, B., Johannessen, T., Olsen, A., Bellerby, R., Wong,
751 C.S., Delille, B., Bates, N.R. and de Baar, H.J.W., 2009. Climatological mean
752 and decadal change in surface ocean $p\text{CO}_2$, and net sea-air CO_2 flux over the
753 global oceans. Deep-Sea Research II, 56(8-10): 554-577.

754 Tans, P.P., Fung, I.Y. and Takahashi, T., 1990. Observational constraints on the global

755 atmospheric CO₂ budget. *Science*, 247(4949): 1431-1438.

756 Tseng, C.-M., Liu, K.K., Gong, G.C., Shen, P.Y. and Cai, W.J., 2011. CO₂ uptake in
757 the East China Sea relying on Changjiang runoff is prone to change.
758 *Geophysical Research Letters*, 38: L24609, doi:10.1029/2011GL049774.

759 Tseng, C.M., Shen, P.-Y. and Liu, K.-K., 2014. Synthesis of observed air-sea CO₂
760 exchange fluxes in the river-dominated East China Sea and improved
761 estimates of annual and seasonal net mean fluxes. *Biogeosciences*, 11:
762 3855-3870.

763 Tsunogai, S., Watanabe, S. and Sato, T., 1999. Is there a "continental shelf pump" for
764 the absorption of atmospheric CO₂? *Tellus B*, 51(3): 701-712.

765 Wang, B.D., Wei, Q.S., Chen, J.F. and Xie, L.P., 2012. Annual cycle of hypoxia off
766 the Changjiang (Yangtze River) Estuary. *Marine Environmental Research*, 77:
767 1-5.

768 Wang, G., Dai, M., Shen, S.S., Bai, Y. and Xu, Y., 2014. Quantifying uncertainty
769 sources in the gridded data of sea surface CO₂ partial pressure. *Journal of*
770 *Geophysical Research-Oceans*, 119(8): 5181-5189.

771 Wang, S.L., Chen, C.T.A., Hong, G.H. and Chung, C.S., 2000. Carbon dioxide and
772 related parameters in the East China Sea. *Continental Shelf Research*, 20(4-5):
773 525-544.

774 Wanninkhof, R., 1992. Relationship between wind speed and gas exchange over the
775 ocean. *Journal of Geophysical Research*, 97(C05): 7373-7382.

776 Wanninkhof, R., Asher, W.E., Ho, D.T., Sweeney, C. and McGillis, W.R., 2009.
777 Advances in quantifying air-sea gas exchange and environmental forcing.
778 *Annual Review of Marine Science*, 1: 213-244.

779 Wanninkhof, R., Doney, S.C., Takahashi, T. and McGillis, W., 2002. The effect of
780 using time-averaged winds on regional air-sea CO₂ fluxes. In: M.A. Donelan
781 (Editor), *Gas Transfer at Water Surfaces*, *Geophys. Monogr. Ser.*, Volume 127.
782 American Geophysical Union, Washington, D.C., doi:10.1029/GM127p0351,
783 pp. 351-357.

784 Weiss, R.F., 1974. Carbon dioxide in water and seawater: the solubility of a non-ideal

785 gas. *Marine Chemistry*, 2: 203-215.

786 Weiss, R.F. and Price, B.A., 1980. Nitrous oxide solubility in water and seawater.
787 *Marine Chemistry*, 8(4): 347-359.

788 Zhai, W., Chen, J., Jin, H., Li, H., Liu, J., He, X. and Bai, Y., 2014. Spring carbonate
789 chemistry dynamics of surface waters in the northern East China Sea: Water
790 mixing, biological uptake of CO₂, and chemical buffering capacity. *Journal of*
791 *Geophysical Research*, 119: 5638-5653.

792 Zhai, W., Dai, M., Chen, B., Guo, X., Li, Q., Shang, S., Zhang, C., Cai, W.-J. and
793 Wang, D., 2013. Seasonal variations of sea-air CO₂ fluxes in the largest
794 tropical marginal sea (South China Sea) based on multiple-year underway
795 measurements. *Biogeosciences*, 10: 7775-7791.

796 Zhai, W.D. and Dai, M.H., 2009. On the seasonal variation of air-sea CO₂ fluxes in
797 the outer Changjiang (Yangtze River) Estuary, East China Sea. *Marine*
798 *Chemistry*, 117(1-4): 2-10.

799 Zhai, W.D., Dai, M.H. and Guo, X.H., 2007. Carbonate system and CO₂ degassing
800 fluxes in the inner estuary of Changjiang (Yangtze) River, China. *Marine*
801 *Chemistry*, 107(3): 342-356.

802

803

804 Table 1 Summary of the five physico-biogeochemical domains categorized in the East China Sea.

805

Domain	Location	Longitude (°E)	Latitude (°N)	Surface area (10 ⁴ km ²)	Description & Characteristics
I	Outer Changjiang Estuary and Changjiang plume	122-126	28.5-33	19.1	Lower estuary beyond the turbidity maximum zone and inner shelf influenced by river plume
II	Zhejiang-Fujian coast	119.33-123.5	25-28.5	4.1	Inner shelf dominated by turbid coastal waters with the influence of river plume primarily in winter.
III	Northern East China Sea	126-128	28.5-33	9.6	Mid- and outer shelf influenced by the Kuroshio. River plume signals visible in flood seasons.
IV	Middle East China Sea	122-128	27-28.5	6.5	Mid- and outer shelf influenced by the Kuroshio.
V	Southern East China Sea	120-125.42	25-27	6.0	Mid- and outer shelf influenced by the Kuroshio and characterized by upwelling northern Taiwan.

806

807

808 Table 2 Summary information of the 24 sampling surveys from 2006 to 2011.

Surveying time	Surveyed zones	Season	Sampling depth/RV	Sampler configuration	References/data source
1-3 January 2006	I	Winter	1.5 m (Fishing boat Hubaoyu 2362)	Modified from Zhai et al. (2007)	Zhai et al., 2007; Zhai and Dai, 2009
18-25 September 2006	I, II	Fall	3 m (Kexue 3)	Modified from Jiang et al. (2008)	This study ^a
14-17 October 2006	I, II, IV	Fall	3 m (Kexue 3)	Modified from Jiang et al. (2008)	This study ^a
20-24 November 2006	I, II	Fall	5 m (Dongfanghong 2)	Modified from Jiang et al. (2008)	This study ^a
2-6 July 2007	I, II, V	Summer	5 m (Dongfanghong 2)	Modified from Jiang et al. (2008)	This study ^a
1-10 November 2007	I, III	Fall	5 m (Dongfanghong 2)	GO8050	Zhai and Dai, 2009
20-30 April 2008	I, II	Spring	5 m (Dongfanghong 2)	GO8050	This study ^a
6-29 August 2008	I, II, IV, V	Summer	5 m (Dongfanghong 2)	GO8050	This study
23-31 December 2008	I, II, V	Winter	5 m (Dongfanghong 2)	GO8050	This study
10-14 January 2009	I, II	Winter	5 m (Dongfanghong 2)	GO8050	This study
15-31 March 2009	I, II, IV, V	Spring	5 m (Dongfanghong 2)	GO8050	This study
6-10 April 2009	I	Spring	1.5 m (Hubaoyu 2362)	Modified from Jiang et al. (2008)	This study
4-30 April 2009	I, II, III, IV, V	Spring	5 m (Dongfanghong 2)	GO8050	This study
1-13 May 2009	I, II, IV, V	Spring	5 m (Dongfanghong 2)	GO 8050	This study
1-3 July 2009	I, II, IV, V	Summer	5 m (Dongfanghong 2)	GO8050	Wang et al. (2014)
17-31 August 2009	I, II, III, IV, V	Summer	5 m (Dongfanghong 2)	GO8050	Wang et al. (2014)
4-31 December 2009	I, II, III, IV, V	Winter	5 m (Dongfanghong 2)	GO8050	This study
1-5 January 2010	II, IV, V	Winter	5 m (Dongfanghong 2)	GO8050	This study
1-6 February 2010	I, II	Winter	5 m (Dongfanghong 2)	GO8050	This study
26-30 November 2010	II, IV, V	Fall	5 m (Dongfanghong 2)	GO8050	This study
1-11 December 2010	I, III, IV	Winter	5 m (Dongfanghong 2)	GO8050	This study
13-15 April 2011	I, IV, V	Spring	5 m (Dongfanghong 2)	GO8050	This study
28-30 May 2011	II, III, IV, V	Spring	5 m (Dongfanghong 2)	GO8050	This study
1-8 June 2011	I, II, III, IV	Summer	5 m (Dongfanghong 2)	GO8050	This study

809 ^a Partially published in Zhai and Dai (2009).

811 Table 3 Data summary of Domain I. Atm. $p\text{CO}_2$ is atmospheric $p\text{CO}_2$; SST is sea surface temperature; SSS is sea surface salinity; F_{CO_2} is the
812 air-sea CO_2 flux, and SD is standard deviation. C_2 is the nonlinearity effect of the short-term variability of wind speeds over a month on the gas
813 transfer velocity, assuming long-term winds followed a Raleigh (Weibull) distribution (Wanninkhof, 1992; Jiang et al., 2008). See text for details.
814 October 2006 and December 2010 were excluded in the calculations of seasonal averages. $p\text{CO}_2$ data are corrected to the reference year 2010.

Season	Period	$p\text{CO}_2$ (μatm)		Atm. $p\text{CO}_2$ (μatm)		$\Delta p\text{CO}_2$ (μatm)		SST ($^{\circ}\text{C}$)		SSS		Wind speed (m s^{-1})		C_2	F_{CO_2} ($\text{mmol m}^{-2} \text{d}^{-1}$)	
		Mean	SD	Mean	SD	Mean	SD	Mean	SD	Mean	SD	Mean	SD		Mean	SD
Winter	23-31 December 2008	356.4	7.2	392.2	0.3	-35.8	7.2	15.0	0.9	31.71	0.86	8.05	0.63	1.24	-7.9	2.2
	4-31 December 2009	352.6	9.3	389.4	0.6	-36.8	9.3	15.7	1.1	32.71	0.96	8.24	0.91	1.19	-7.7	4.0
	1-3 January 2006	360.7	17.5	395.4	1.6	-34.7	17.5	12.2	1.1	30.28	4.28	8.12	0.82	1.14	-6.5	6.9
	1-14 January 2009	341.4	2.6	399.3	0.4	-58.0	2.6	8.1	0.8	29.98	0.73	8.42	0.89	1.20	-13.5	1.9
	1-5 January 2010	-	-	-	-	-	-	-	-	-	-	7.95	0.85	1.22	-	-
	1-6 February 2010	329.8	6.6	395.7	0.2	-65.9	6.6	11.3	0.7	32.65	0.45	7.86	0.72	1.21	-13.3	3.8
	1-11 December 2010	384.2	19.7	390.3	0.5	-6.1	19.7	18.0	0.6	33.01	0.65	9.11	0.67	1.23	-1.6	7.5
	Seasonal average		348.2	11.1	394.4	0.9	-46.2	11.1	12.4	1.0	31.47	2.28	8.11	0.89	1.20	-9.8
Spring	15-31 March 2009	359.4	13.4	391.9	0.4	-32.5	13.5	12.0	0.7	29.89	1.97	7.68	0.93	1.16	-5.8	6.2
	20-30 April 2008	315.6	53.0	396.5	0.7	-81.0	53.0	16.0	1.7	29.99	7.03	5.83	0.41	1.27	-9.9	6.0
	4-30 April 2009	303.5	28.2	395.9	0.3	-92.3	28.2	15.1	0.8	31.21	0.79	5.94	0.42	1.26	-11.5	4.6
	6-10 April 2009	286.3	101.7	398.6	0.7	-112.3	101.7	13.5	1.1	29.83	6.85	5.94	0.42	1.26	-14.0	11.1
	12-15 April 2011	295.8	46.0	398.9	0.4	-103.1	46.0	12.4	0.7	32.42	0.62	6.25	0.31	1.25	-14.0	8.8
	1-20 May 2009	292.7	41.2	388.3	0.4	-95.6	41.2	17.8	0.6	30.28	1.45	5.43	0.26	1.20	-8.9	6.3
	26-31 May 2011	-	-	-	-	-	-	-	-	-	-	5.79	0.23	1.21	-	-
Seasonal average		308.9	59.9	395.0	0.5	-86.1	59.9	14.5	1.1	30.60	4.55	6.12	0.52	1.23	-10.7	8.2
Summer	1-12 July 2009	357.2	56.0	369.5	0.6	-12.3	56.0	23.3	0.6	30.47	1.18	6.40	0.52	1.18	-1.6	9.3

	2-6 July 2007	292.7	56.1	374.9	0.5	-82.1	56.1	24.5	0.7	30.69	1.50	5.57	0.77	1.27	-8.9	7.3
	6-29 August 2008	339.8	77.9	374.6	0.5	-34.8	77.9	28.0	0.6	31.02	1.16	5.41	0.50	1.21	-3.3	12.6
	17-31 August 2009	293.8	64.5	362.8	0.6	-69.0	64.5	28.6	0.7	30.38	1.52	6.13	0.32	1.22	-8.4	9.7
	1-19 June 2011	302.4	64.6	387.6	0.7	-85.2	64.6	19.7	0.7	32.08	0.76	5.85	0.49	1.27	-10.2	8.0
	Seasonal average	317.2	71.9	373.9	0.6	-56.7	71.9	24.8	0.7	30.93	1.41	5.87	0.60	1.23	-6.5	10.7
Fall	18-25 September 2006	387.8	50.0	374.9	0.7	12.9	50.0	25.3	0.3	33.34	1.08	7.01	0.56	1.19	2.7	5.8
	14-18 October 2006	364.3	65.6	382.8	0.4	-18.5	65.6	25.2	0.4	33.47	1.67	6.12	0.61	1.13	-1.9	5.5
	20-24 November 2006	396.9	23.6	386.3	0.3	10.6	23.6	20.9	0.4	32.93	0.46	7.74	0.69	1.17	1.9	3.7
	1-10 November 2007	395.7	14.4	385.5	0.3	10.3	14.4	22.7	0.3	33.95	0.17	8.14	1.06	1.13	1.9	6.8
	26-30 November 2010	-	-	-	-	-	-	-	-	-	-	6.73	0.74	1.22	-	-
	Seasonal average	393.5	40.4	382.2	0.6	11.3	40.4	23.0	0.5	33.41	0.84	7.41	0.91	1.17	2.2	6.8
Annual average		341.9	59.2	386.4	0.8	-44.4	59.2	18.7	1.0	31.60	3.08	6.88	0.86	1.21	-6.2	9.1

815

816

817

818 Table 4 Data summary of Domain II. Atm. $p\text{CO}_2$ is atmospheric $p\text{CO}_2$; SST is sea surface temperature; SSS is sea surface salinity; F_{CO_2} is the
819 air-sea CO_2 flux, and SD is standard deviation. C_2 is the nonlinearity effect of the short-term variability of wind speeds over a month on the gas
820 transfer velocity, assuming long-term winds followed a Raleigh (Weibull) distribution (Wanninkhof, 1992; Jiang et al., 2008). See text for details.
821 October 2006 and December 2010 were excluded in the calculations of seasonal averages. $p\text{CO}_2$ data are corrected to the reference year 2010.

Season	Period	$p\text{CO}_2$ (μatm)		Atm. $p\text{CO}_2$ (μatm)		$\Delta p\text{CO}_2$ (μatm)		SST ($^{\circ}\text{C}$)		SSS		Wind speed (m s^{-1})		C_2	F_{CO_2} ($\text{mmol m}^{-2} \text{d}^{-1}$)			
		Mean	SD	Mean	SD	Mean	SD	Mean	SD	Mean	SD	Mean	SD		Mean	SD		
Winter	23-31 December 2008	350.3	8.0	389.0	0.9	-38.6	8.1	16.2	1.7	30.59	1.38	8.56	0.99	1.18	-8.7	1.4		
	4-31 December 2009	343.8	7.7	389.8	0.6	-46.1	7.7	19.4	0.7	34.26	0.26	8.02	0.74	1.17	-8.7	0.3		
	1-3 January 2006	-	-	-	-	-	-	-	-	-	-	-	-	8.71	0.88	1.11	-	-
	1-14 January 2009	347.7	4.5	395.0	0.3	-47.3	4.5	12.7	0.5	29.64	0.47	9.01	1.02	1.12	-10.9	0.9		
	1-5 January 2010	353.0	9.3	391.4	1.5	-38.4	9.4	16.6	1.6	32.38	0.91	7.90	0.76	1.22	-7.8	1.9		
	1-6 February 2010	352.4	7.2	392.5	0.5	-40.1	7.2	12.7	0.7	31.19	0.49	7.98	0.59	1.20	-8.3	1.6		
	1-11 December 2010	-	-	-	-	-	-	-	-	-	-	-	-	7.83	0.71	1.28	-	-
	Seasonal average	349.4	8.4	391.5	1.0	-42.1	8.4	15.5	1.3	31.61	0.90	8.36	0.92	1.18	-8.9	1.4		
Spring	15-31 March 2009	308.5	13.4	389.6	0.5	-81.1	13.4	18.5	0.8	34.01	0.23	8.30	0.69	1.14	-15.7	2.6		
	20-30 April 2008	331.2	22.5	392.0	1.1	-60.9	22.6	21.8	1.7	33.83	0.82	6.38	0.53	1.19	-7.5	3.3		
	4-30 April 2009	312.4	11.7	392.1	0.3	-79.7	11.7	20.1	0.2	34.01	0.06	7.00	0.97	1.17	-11.5	1.7		
	6-10 April 2009	-	-	-	-	-	-	-	-	-	-	7.00	0.97	1.17	-	-		
	12-15 April 2011	-	-	-	-	-	-	-	-	-	-	6.57	0.52	1.24	-	-		
	1-20 May 2009	290.6	35.8	386.7	0.7	-96.1	35.8	21.5	1.1	32.63	1.47	5.67	0.56	1.18	-9.4	4.0		
	26-31 May 2011	323.1	11.9	394.8	0.9	-71.7	11.9	22.2	0.2	32.63	0.56	6.26	0.42	1.23	-9.1	3.4		

	Seasonal average	313.2	23.7	391.1	0.8	-77.9	23.7	20.8	1.1	33.42	0.89	6.74	0.75	1.19	-10.7	3.5
Summer	1-12 July 2009	361.4	16.9	367.1	0.4	-5.7	16.9	26.6	0.3	33.51	0.22	6.33	0.51	1.19	-0.7	2.0
	2-6 July 2007	346.9	11.8	373.5	0.4	-26.6	11.8	26.5	0.8	33.81	0.31	6.86	0.59	1.21	-3.9	1.6
	6-29 August 2008	397.3	2.9	374.7	0.3	22.6	2.9	28.8	0.5	33.40	0.28	5.56	0.40	1.23	2.3	0.3
	17-31 August 2009	363.3	38.0	362.8	0.3	0.5	38.0	28.8	0.3	33.06	0.47	6.19	0.27	1.52	0.1	6.0
	1-19 June 2011	318.6	0.3	387.7	1.6	-69.1	1.6	21.2	0.0	33.40	0.02	6.78	0.43	1.18	-9.5	0.0
	Seasonal average	357.5	21.7	373.2	0.9	-15.7	21.7	26.4	0.5	33.44	0.33	6.34	0.51	1.27	-2.4	3.3
Fall	18-25 September 2006	407.5	14.2	374.8	0.6	32.8	14.2	26.1	0.1	33.04	0.31	7.28	0.77	1.19	5.2	3.0
	14-18 October 2006	308.4	25.3	381.6	0.2	-73.3	25.3	25.7	0.1	33.37	0.43	7.17	1.07	1.12	-10.1	4.7
	20-24 November 2006	377.7	8.1	377.7	8.1	0.0	11.4	23.1	0.3	33.23	0.34	6.97	0.75	1.18	-1.0	1.2
	1-10 November 2007	-	-	-	-	-	-	-	-	-	-	10.81	1.40	1.07	-	-
	26-30 November 2010	378.5	16.4	388.5	0.6	-10.1	16.5	19.5	1.0	32.00	1.40	9.01	1.29	1.10	-2.1	4.8
	Seasonal average	387.9	16.4	380.3	5.7	7.6	17.4	22.9	0.8	32.76	1.05	8.52	1.26	1.13	0.7	4.1
Annual average		352.0	21.4	384.0	3.4	-32.0	21.6	21.4	1.1	32.81	0.97	7.49	1.04	1.19	-5.3	3.7

822

823

824

825 Table 5 Data summary of Domain III. Atm. $p\text{CO}_2$ is atmospheric $p\text{CO}_2$; SST is sea surface temperature; SSS is sea surface salinity; F_{CO_2} is the
826 air-sea CO_2 flux, and SD is standard deviation. C_2 is the nonlinearity effect of the short-term variability of wind speeds over a month on the gas
827 transfer velocity, assuming long-term winds followed a Raleigh (Weibull) distribution (Wanninkhof, 1992; Jiang et al., 2008). See text for details.
828 October 2006 and December 2010 were excluded in the calculations of seasonal averages. $p\text{CO}_2$ data are corrected to the reference year 2010.

Season	Period	$p\text{CO}_2$ (μatm)		Atm. $p\text{CO}_2$ (μatm)		$\Delta p\text{CO}_2$ (μatm)		SST ($^{\circ}\text{C}$)		SSS		Wind speed (m s^{-1})		C_2	F_{CO_2} ($\text{mmol m}^{-2} \text{d}^{-1}$)	
		Mean	SD	Mean	SD	Mean	SD	Mean	SD	Mean	SD	Mean	SD		Mean	SD
Winter	23-31 December 2008	-	-	-	-	-	-	-	-	-	-	8.21	0.16	1.25	-	-
	4-31 December 2009	340.1	8.8	385.9	0.5	-45.7	8.8	19.6	0.8	34.38	0.15	8.86	0.30	1.18	-10.8	1.4
	1-3 January 2006	-	-	-	-	-	-	-	-	-	-	8.79	0.38	1.13	-	-
	1-14 January 2009	-	-	-	-	-	-	-	-	-	-	9.21	0.25	1.18	-	-
	1-5 January 2010	-	-	-	-	-	-	-	-	-	-	8.48	0.36	1.21	-	-
	1-6 February 2010	-	-	-	-	-	-	-	-	-	-	8.39	0.31	1.19	-	-
	1-11 December 2010	335.2	9.2	387.3	0.5	-52.2	9.2	22.3	0.5	34.42	0.04	9.79	0.51	1.20	-15.3	5.2
	Seasonal average	340.1	8.8	385.9	0.5	-45.7	8.8	19.6	0.8	34.38	0.15	8.66	0.30	1.19	-10.8	1.4
Spring	15-31 March 2009	-	-	-	-	-	-	-	-	-	-	8.81	0.36	1.13	-	-
	20-30 April 2008	-	-	-	-	-	-	-	-	-	-	6.68	0.38	1.21	-	-
	4-30 April 2009	289.5	10.4	396.2	0.8	-106.7	10.4	17.8	1.2	34.14	0.27	6.95	0.62	1.26	-17.8	3.1
	6-10 April 2009	-	-	-	-	-	-	-	-	-	-	6.95	0.62	1.26	-	-
	12-15 April 2011	-	-	-	-	-	-	-	-	-	-	6.93	0.27	1.24	-	-
	1-20 May 2009	-	-	-	-	-	-	-	-	-	-	6.17	0.41	1.20	-	-
	26-31 May 2011	-	-	-	-	-	-	-	-	-	-	5.61	0.25	1.25	-	-

	Seasonal average	289.5	10.4	396.2	0.8	-106.7	10.4	17.8	1.2	34.14	0.27	6.87	0.62	1.22	-17.8	3.1
Summer	1-12 July 2009	-	-	-	-	-	-	-	-	-	-	6.69	0.23	1.14	-	-
	2-6 July 2007	-	-	-	-	-	-	-	-	-	-	5.94	0.61	1.40	-	-
	6-29 August 2008	-	-	-	-	-	-	-	-	-	-	6.23	0.39	1.18	-	-
	17-31 August 2009	378.3	10.2	362.1	0.3	16.2	10.2	29.4	0.3	33.12	0.49	5.59	0.25	1.28	1.8	3.7
	1-19 June 2011	304.0	14.5	386.6	1.2	-82.6	14.5	19.3	0.8	33.34	0.35	6.10	0.65	1.28	-10.9	1.6
	Seasonal average	341.1	17.7	374.3	1.2	-33.2	17.8	24.3	0.9	33.23	0.60	6.11	0.52	1.26	-4.6	4.0
Fall	18-25 September 2006	-	-	-	-	-	-	-	-	-	-	7.08	0.88	1.20	-	-
	14-18 October 2006	-	-	-	-	-	-	-	-	-	-	7.03	0.59	1.14	-	-
	20-24 November 2006	-	-	-	-	-	-	-	-	-	-	7.82	0.52	1.17	-	-
	1-10 November 2007	367.3	8.6	384.9	0.3	-17.6	8.6	23.7	0.3	34.19	0.06	8.96	0.50	1.11	-3.7	5.1
	26-30 November 2010	-	-	-	-	-	-	-	-	-	-	7.40	0.20	1.17	-	-
	Seasonal average	367.3	8.6	384.9	0.3	-17.6	8.6	23.7	0.3	34.19	0.06	7.82	0.50	1.16	-3.7	5.1
Annual average		334.5	13.8	385.3	0.9	-50.8	13.8	21.4	1.0	33.98	0.39	7.36	0.57	1.21	-9.2	4.2

829

830

831

832 Table 6 Data summary of Domain IV. Atm. $p\text{CO}_2$ is atmospheric $p\text{CO}_2$; SST is sea surface temperature; SSS is sea surface salinity; F_{CO_2} is the
833 air-sea CO_2 flux, and SD is standard deviation. C_2 is the nonlinearity effect of the short-term variability of wind speeds over a month on the gas
834 transfer velocity, assuming long-term winds followed a Raleigh (Weibull) distribution (Wanninkhof, 1992; Jiang et al., 2008). See text for details.
835 October 2006 and December 2010 were excluded in the calculations of seasonal averages. $p\text{CO}_2$ data are corrected to the reference year 2010.

Season	Period	$p\text{CO}_2$ (μatm)		Atm. $p\text{CO}_2$ (μatm)		$\Delta p\text{CO}_2$ (μatm)		SST ($^{\circ}\text{C}$)		SSS		Wind speed (m s^{-1})		C_2	F_{CO_2} ($\text{mmol m}^{-2} \text{d}^{-1}$)	
		Mean	SD	Mean	SD	Mean	SD	Mean	SD	Mean	SD	Mean	SD		Mean	SD
Winter	23-31 December 2008	335.5	3.8	387.5	0.3	-52.0	3.8	20.6	0.6	34.04	0.32	8.85	0.34	1.16	-11.8	0.9
	4-31 December 2009	339.1	5.1	387.3	0.7	-48.2	5.1	20.1	0.8	34.55	0.08	8.60	0.19	1.19	-10.8	1.6
	1-3 January 2006	-	-	-	-	-	-	-	-	-	-	9.02	0.30	1.11	-	-
	1-14 January 2009	-	-	-	-	-	-	-	-	-	-	9.36	0.45	1.16	-	-
	1-5 January 2010	347.5	2.3	389.3	0.2	-41.8	2.3	19.1	0.3	34.46	0.12	8.42	0.30	1.19	-9.0	0.5
	1-6 February 2010	-	-	-	-	-	-	-	-	-	-	9.06	0.14	1.16	-	-
	1-11 December 2010	331.2	4.0	388.7	0.5	-57.5	4.1	22.6	0.5	34.46	0.04	8.96	0.17	1.22	-14.6	1.3
Seasonal average	340.7	4.8	388.0	0.6	-47.3	4.8	19.9	0.8	34.35	0.25	8.89	0.33	1.17	-10.6	1.3	
Spring	15-31 March 2009	305.8	13.5	387.6	0.7	-81.8	13.5	21.3	1.0	34.36	0.10	9.15	0.20	1.13	-18.7	3.1
	20-30 April 2008	-	-	-	-	-	-	-	-	-	-	7.07	0.21	1.17	-	-
	4-30 April 2009	326.3	16.0	391.6	0.8	-65.4	16.1	21.5	1.3	33.99	0.52	7.57	0.37	1.15	-10.6	0.7
	6-10 April 2009	-	-	-	-	-	-	-	-	-	-	7.57	0.37	1.15	-	-
	12-15 April 2011	317.3	17.5	396.3	1.0	-79.0	17.6	18.4	1.5	34.43	0.34	6.88	0.08	1.18	-11.3	0.9
	1-20 May 2009	300.1	20.1	388.6	0.8	-88.6	20.1	21.0	1.3	33.81	0.44	5.98	0.22	1.16	-9.2	2.8
	26-31 May 2011	342.8	7.3	394.0	0.1	-51.3	7.3	22.7	0.4	34.24	0.18	6.17	0.35	1.21	-6.1	0.6

	Seasonal average	318.4	17.3	391.6	0.8	-73.2	17.4	21.0	1.3	34.17	0.39	7.20	0.30	1.16	-11.2	2.2
Summer	1-12 July 2009	388.7	5.0	366.7	0.2	22.0	5.0	27.1	0.3	33.95	0.14	6.75	0.12	1.14	2.8	0.6
	2-6 July 2007	375.0	12.5	372.9	0.2	2.1	12.5	28.2	0.3	33.76	0.12	6.95	0.25	1.27	0.4	2.1
	6-29 August 2008	392.7	2.4	374.7	0.2	18.1	2.4	28.7	0.2	33.48	0.17	5.51	0.16	1.18	1.6	0.2
	17-31 August 2009	400.4	5.8	361.0	0.3	39.4	5.8	29.5	0.3	33.66	0.13	6.05	0.23	1.47	6.7	2.1
	1-19 June 2011	345.1	9.8	386.6	1.2	-41.5	9.9	22.9	0.7	34.18	0.25	7.33	0.24	1.17	-6.5	0.2
	Seasonal average	380.4	8.9	372.4	0.6	8.0	8.9	27.3	0.4	33.81	0.19	6.52	0.23	1.25	1.0	1.5
Fall	18-25 September 2006	-	-	-	-	-	-	-	-	-	-	6.39	0.42	1.26	-	-
	14-18 October 2006	327.6	35.5	381.8	0.2	-54.2	35.5	25.7	0.3	34.18	0.33	7.56	0.28	1.10	-7.9	0.1
	20-24 November 2006	-	-	-	-	-	-	-	-	-	-	7.06	0.14	1.18	-	-
	1-10 November 2007	-	-	-	-	-	-	-	-	-	-	10.37	0.53	1.08	-	-
	26-30 November 2010	336.4	2.4	386.8	0.3	-50.4	2.4	21.8	0.2	34.42	0.04	8.39	0.40	1.11	-9.3	0.5
	Seasonal average	336.4	2.4	386.8	0.3	-50.4	2.4	21.8	0.2	34.42	0.04	8.05	0.40	1.15	-9.3	0.5
Annual average		344.0	11.7	384.7	0.7	-40.7	11.7	22.5	0.9	34.18	0.29	7.66	0.37	1.18	-7.5	1.7

836

837

838

839 Table 7 Data summary of Domain V. Atm. $p\text{CO}_2$ is atmospheric $p\text{CO}_2$; SST is sea surface temperature; SSS is sea surface salinity; F_{CO_2} is the
840 air-sea CO_2 flux, and SD is standard deviation. C_2 is the nonlinearity effect of the short-term variability of wind speeds over a month on the gas
841 transfer velocity, assuming long-term winds followed a Raleigh (Weibull) distribution (Wanninkhof, 1992; Jiang et al., 2008). See text for details.
842 October 2006 and December 2010 were excluded in the calculations of seasonal averages. $p\text{CO}_2$ data are corrected to the reference year 2010.

Season	Period	$p\text{CO}_2$ (μatm)		Atm $p\text{CO}_2$ (μatm)		$\Delta p\text{CO}_2$ (μatm)		SST ($^\circ\text{C}$)		SSS		Wind speed (m s^{-1})		C_2	F_{CO_2} ($\text{mmol m}^{-2} \text{d}^{-1}$)	
		Mean	SD	Mean	SD	Mean	SD	Mean	SD	Mean	SD	Mean	SD	Mean	Mean	SD
Winter	23-31 December 2008	340.5	4.3	386.5	0.5	-46.0	4.36	21.2	0.9	34.00	0.17	9.21	0.52	1.14	-10.9	1.0
	4-31 December 2009	340.8	2.9	387.3	0.3	-46.5	2.92	23.1	0.3	34.66	0.06	8.74	0.44	1.16	-10.2	2.4
	1-3 January 2006	-	-	-	-	-	-	-	-	-	-	9.30	0.46	1.11	-	-
	1-14 January 2009	-	-	-	-	-	-	-	-	-	-	10.02	0.49	1.09	-	-
	1-5 January 2010	349.6	11.2	389.3	0.2	-39.7	11.21	21.0	1.1	34.58	0.04	8.78	0.50	1.17	-9.0	2.5
	1-6 February 2010	-	-	-	-	-	-	-	-	-	-	8.39	0.80	1.20	-	-
	1-11 December 2010	-	-	-	-	-	-	-	-	-	-	8.41	0.49	1.24	-	-
	Seasonal average	343.6	8.7	387.7	0.5	-44.1	8.75	21.7	1.0	34.41	0.13	9.07	0.60	1.16	-10.0	2.5
Spring	15-31 March 2009	326.5	20.6	386.7	1.0	-60.3	20.61	24.2	1.8	34.21	0.09	8.82	0.56	1.12	-12.5	4.3
	20-30 April 2008	-	-	-	-	-	-	-	-	-	-	6.96	0.47	1.17	-	-
	4-30 April 2009	354.9	6.4	387.8	1.6	-32.9	6.59	24.9	2.2	34.32	0.06	8.03	0.32	1.12	-5.6	1.1
	6-10 April 2009	-	-	-	-	-	-	-	-	-	-	8.03	0.32	1.12	-	-
	12-15 April 2011	339.8	7.0	392.5	1.0	-52.7	7.08	24.1	0.8	34.70	0.06	6.88	0.33	1.17	-7.2	-7.2
	1-20 May 2009	342.8	7.6	385.3	0.9	-42.5	7.70	24.0	1.2	34.27	0.08	6.09	0.27	1.14	-4.4	0.9
	26-31 May 2011	362.0	6.0	394.0	0.1	-32.1	6.04	24.6	0.7	34.22	0.11	6.46	0.33	1.21	-4.2	0.4

	Seasonal average	345.2	12.3	389.3	1.2	-44.1	12.39	24.4	1.6	34.34	0.09	7.32	0.41	1.15	-6.8	4.3
Summer	1-12 July 2009	380.5	12.9	366.5	0.5	14.0	12.96	27.6	1.0	34.00	0.20	6.52	0.43	1.23	1.9	0.2
	2-6 July 2007	388.5	11.6	373.9	1.6	14.7	11.67	28.4	1.8	34.18	0.28	6.14	0.64	1.26	1.9	0.2
	6-29 August 2008	374.3	10.2	374.4	0.4	-0.1	10.23	28.6	0.4	33.05	0.33	5.33	0.31	1.24	-0.0	0.2
	17-31 August 2009	378.8	19.8	363.7	0.7	15.0	19.80	28.1	0.7	33.53	0.22	5.91	0.43	1.70	3.2	4.8
	1-19 June 2011	-	-	-	-	-	-	-	-	-	-	6.90	0.55	1.19	-	-
	Seasonal average	380.5	16.3	369.6	1.1	10.9	16.34	28.2	1.3	33.69	0.30	6.16	0.54	1.32	1.8	2.8
Fall	18-25 September 2006	-	-	-	-	-	-	-	-	-	-	6.93	0.60	1.19	-	-
	14-18 October 2006	-	-	-	-	-	-	-	-	-	-	7.80	0.52	1.09	-	-
	20-24 November 2006	-	-	-	-	-	-	-	-	-	-	7.27	0.38	1.16	-	-
	1-10 November 2007	-	-	-	-	-	-	-	-	-	-	11.42	0.66	1.06	-	-
	26-30 November 2010	347.9	6.1	385.9	0.6	-38.1	6.16	24.6	0.8	34.43	0.07	9.46	0.75	1.08	-8.4	2.0
	Seasonal average	347.9	6.1	385.9	0.6	-38.1	6.16	24.6	0.8	34.43	0.07	8.77	0.75	1.12	-8.4	2.0
Annual average		354.3	13.3	383.1	1.0	-28.8	13.35	24.7	1.4	34.22	0.20	7.83	0.68	1.19	-5.9	3.4

843

844

845

846 Table 8 Comparison of air-sea CO₂ fluxes in the East China Sea shelf

847

Study area	Season	Methods*	Wind speed	k [§]	FCO ₂ (mmol m ⁻² d ⁻¹)	FCO ₂ _S(07) [#] (mmol m ⁻² d ⁻¹)	Data source
Domain I	Spring	1	Short-term	W92_S	-8.8±5.8	-7.7±5.1	Zhai and Dai (2009)
	Spring	1	Monthly	S07		-10.7±8.2	This study
	Summer	1	Short-term	W92_S	-4.9±4.0	-4.3±3.5	Zhai and Dai (2009)
	Summer	1	Monthly	S07		-6.5±10.7	This study
	Fall	1	Short-term	W92_S	2.9±2.5	2.5±2.2	Zhai and Dai (2009)
	Fall	1	Monthly	S07		2.2±6.8	This study
	Winter	1	Short-term	W92_S	-10.4±2.3	-9.1±2.0	Zhai and Dai (2009)
	Winter	1	Monthly	S07		-9.8±4.6	This study
	Annual	1	Short-term	W92_S	-5.2±3.6	-4.5±3.1	Zhai and Dai (2009)
	Annual	1	Monthly	S07		-6.2±9.1	This study
Domains I and III	Spring	1	Monthly	W92_L	-5.0±1.6	-4.2±1.3	Shim et al. (2007)
	Spring	1	Daily	W92_S	-6.8±4.3	-5.9±3.7	Kim et al. (2013)
	Spring	1	Monthly	S07		-13.0±6.6	This study
	Summer	1	Daily	W92_S	-6.6±8.5	-5.7±7.4	Kim et al. (2013)
	Summer	1	Monthly	S07		-5.8±8.5	This study
	Fall	1	Monthly	W92_L	1.1±2.9	0.9±2.4	Shim et al. (2007)
	Fall	1	Daily	W92_S	0.8±7.3	0.7±6.4	Kim et al. (2013)
	Fall	1	Monthly	S07		0.2±6.2	This study

	Winter	1	Daily	W92_S	-12±4.1	-10.5±3.6	Kim et al. (2013)
	Winter	1	Monthly	S07		-10.1±3.6	This study
	Annual	4	-	-	-8	-	Tsunogai et al. (1999)
	Annual	1	Daily	W92_S	-6.0±5.8	-5.2±5.0	Kim et al. (2013)
	Annual	1	Monthly	S07		-7.2±6.2	This study
Domains I, III and IV	Summer	2	-	L&M86; T90	-1.8 to -4.8	-	Wang et al. (2000)
	Summer	1	Monthly	S07		-4.6±5.9	This study
Domains II, IV and V	Spring	2	Long-term	-	-5.8±7.7	-	Peng et al. (1999)
	Spring	1	Monthly	S07		-9.5±2.0	This study
	Spring	3	Monthly	S07	-	-8.2±2.1	Tseng et al. (2014)
	Spring	3	Long-term	W92_L	-11.5±2.5	-9.6±2.1	Tseng et al. (2011)
	Spring	1	Monthly	S07		-11.7±3.6	This study
ECS shelf	Summer	1	Daily	S07		-2.4±3.1	Chou et al. (2009)
	Summer	3	Long-term	W92_L	-1.9±1.4	-1.6±1.2	Tseng et al. (2011)
	Summer	3	Monthly	S07		-2.5±3.0	Tseng et al. (2014)
	Summer	1	Monthly	S07		-3.5±4.6	This study
	Fall	3	Long-term	W92_L	-2.2±3.0	-1.8±2.5	Tseng et al. (2011)
	Fall		Monthly	S07		-0.8±1.9	Tseng et al. (2014)
	Fall	1	Monthly	S07		-2.3±3.1	This study
	Winter	1	Monthly	W92_L	-13.7±5.7	-11.4±4.7	Chou et al. (2011)
	Winter	3	Long-term	W92_L	-9.3±1.9	-7.7±1.6	Tseng et al. (2011)
	Winter	3	Monthly	S07		-5.5±1.6	Tseng et al. (2014)
	Winter	1	Monthly	S07		-10.0±2.0	This study

Annual	3	Long-term	W92_L	-6.3±1.1	-5.2±0.9	Tseng et al. (2011)
Annual	3	Monthly	S07		-3.8±1.1	Tseng et al. (2014)
Annual	1	Monthly	S07		-6.9±4.0	This study

848 * Methods

849 1: $p\text{CO}_2$ measurements and gas transfer algorithms with wind speeds;

850 2: $p\text{CO}_2$ calculated from DIC and TA and gas transfer algorithms with wind speeds;

851 3: $p\text{CO}_2$ algorithms (with Changjiang discharge and SST) and gas transfer algorithms with wind speeds;

852 4: $p\text{CO}_2$ measurements and algorithms (with SST, SSS and phosphate) and given gas transfer velocity;

853 §: W92_S is Wanninkhof (1992) algorithm for short-term wind speeds; W92_L is Wanninkhof (1992) algorithm for long-term (or monthly
854 average) wind speeds; S07 is Sweeney et al. (2007) algorithm; L&M86 is Liss and Merlivat (1986) algorithm; T90 is Tans (1990) algorithm.

855 #: FCO_2 data were calculated (or recalculated) with the Sweeney et al. (2007) gas transfer algorithm with wind speed.

856

857

858

859

860

861

862 Figure captions

863 Fig. 1 Map of the East China Sea showing the study area. Areas framed with black
864 solid lines indicate the five physico-biogeochemical domains categorized in this study
865 to better constrain the spatial and temporal variability of CO₂ fluxes, as detailed in
866 Table 1. The arrows show the direction of the Kuroshio Current. The area framed by
867 pink dashed lines shows the study area of Shim et al. (2007) and Kim et al. (2013); by
868 brown dashed lines of Zhai and Dai (2009); by blue dashed lines of Wang et al. (2000);
869 by red dashed lines of Chou et al. (2009a; 2011) and Tseng et al. (2011); and by black
870 dashed lines of Peng et al. (1999). The solid brown line is the PN line which was the
871 major survey track of Tsunogai et al. (1999). Note that the color bar for the depth
872 scale is non-linear.

873 Fig. 2 Spatial distribution of surface water pCO₂ (µatm) in the East China Sea in the
874 12 month surveys of 2006 to 2011. The framed areas show the five
875 physico-biogeochemical domains. Data are corrected to the reference year 2010.

876 Fig. 3 Spatial distribution of sea surface temperature (SST) in the East China Sea in
877 the 12 month surveys of 2006 to 2011. The climatology (from 2003 to 2013)
878 monthly-mean SST were calculated based on the monthly mean SST obtained from
879 the NASA ocean color website (<http://oceancolor.gsfc.nasa.gov>), which were retrieved
880 with the Moderate Resolution Imaging Spectroradiometer (MODIS) on board the
881 Aqua satellite. The 4 µm nighttime SST products were used here. The SST data in the
882 track were measured during the surveys. The framed areas show the five
883 physico-biogeochemical domains. In panel M, the SST data in the track were
884 measured during the December 2010 cruise while the background is the climatology
885 (from 2003 to 2013) monthly-mean SST.

886 Fig. 4 Seasonal variations of sea surface temperature (SST, A) and salinity (SSS, B) in
887 Domain I (red curve), Domain II (blue curve), Domain III (pink curve), Domain IV
888 (green curve) and Domain V (black curve). The mean SST data were retrieved with
889 the Moderate Resolution Imaging Spectroradiometer (MODIS) on board the Aqua

890 satellite from NASA ocean color website (<http://oceancolor.gsfc.nasa.gov>). The 4 μm
891 nighttime SST products were used here. The mean SSS were based on the data
892 presented in Tables 3-7. The data during each survey are shown as mean \pm standard
893 deviation.

894 Fig. 5 Temporal distribution of atmospheric CO₂ concentrations based on ship-board
895 measurements during the cruise to the East China Sea (arithmetic average, red solid
896 dots) and its comparison with the measurements at 21 m above sea level, at Tae-ahn
897 Peninsula (blue solid line) (36.7376 °N, 126.1328 °E, Republic of Korea,
898 <http://www.esrl.noaa.gov/gmd/dv/site>) and at Mauna Loa Observatory at Hawaii (pink
899 solid line, Scripps CO₂ program, <http://scrippsco2.ucsd.edu>). The error bars are the
900 standard deviations. The CO₂ concentrations in this plot are the original values in the
901 year of the observations.

902 Fig. 6 Distribution of seasonal average and standard deviations (SD) of $p\text{CO}_2$ in $1^\circ \times 1^\circ$
903 grids on the East China Sea shelf. The framed areas show the five
904 physico-biogeochemical domains. Panel A-1 and A-2 are the result of the winter
905 cruises excluding December 2010; panels D-1 and D-2 are results of the fall cruises
906 excluding October 2006. Data are corrected to the reference year 2010. The surveys
907 conducted in October 2006 and November 2010 were not excluded in the seasonal
908 average calculations and were presented separately, which was due mainly to the
909 abnormal characters of these two surveys. See detail in the text.

910 Fig. 7 CO₂ fluxes and seasonal variations in the East China Sea. The error bars are the
911 standard deviations.

912 Fig. 8 Relationships of $p\text{CO}_2$ and $Np\text{CO}_2$ (normalized $p\text{CO}_2$ to 21 °C) of the surface
913 water with sea surface temperature (SST). Panels A-1 and B-1 are Domain I; panels
914 A-2 and B-2 are Domain II; panels A-3 and B-3 are Domain III; panels A-4 and B-4
915 are Domain IV; panels A-5 and B-5 are Domain V. The dashed lines in panels A-1 to
916 A-5 represent $250 \times \exp((\text{SST}-21) \times 0.0423)$ and $400 \times \exp((\text{SST}-21) \times 0.0423)$ μatm , in
917 which 250 and 400 μatm are the lower and higher limits of $Np\text{CO}_2$ in Domains IV and

918 V (see details in the text). $p\text{CO}_2$ and $Np\text{CO}_2$ values are in the year of observations.

919 Fig. 9 Relationships of $p\text{CO}_2$ of the surface water with sea surface salinity (SSS).

920 Panels A, B, C, D and E are Domains I to V, respectively. $p\text{CO}_2$ values are in the year
921 of observations.

922 Fig. 10 Relationships of $p\text{CO}_2$ and $Np\text{CO}_2$ (normalized $p\text{CO}_2$ to 21 °C) with

923 chlorophyll a (Chl-*a*) concentration. The data of Chl-*a* concentration in surface water

924 were unpublished data from Dr. Jun Sun. The spring surveys include April and May

925 2011; the summer surveys include July and August 2009; the fall surveys include

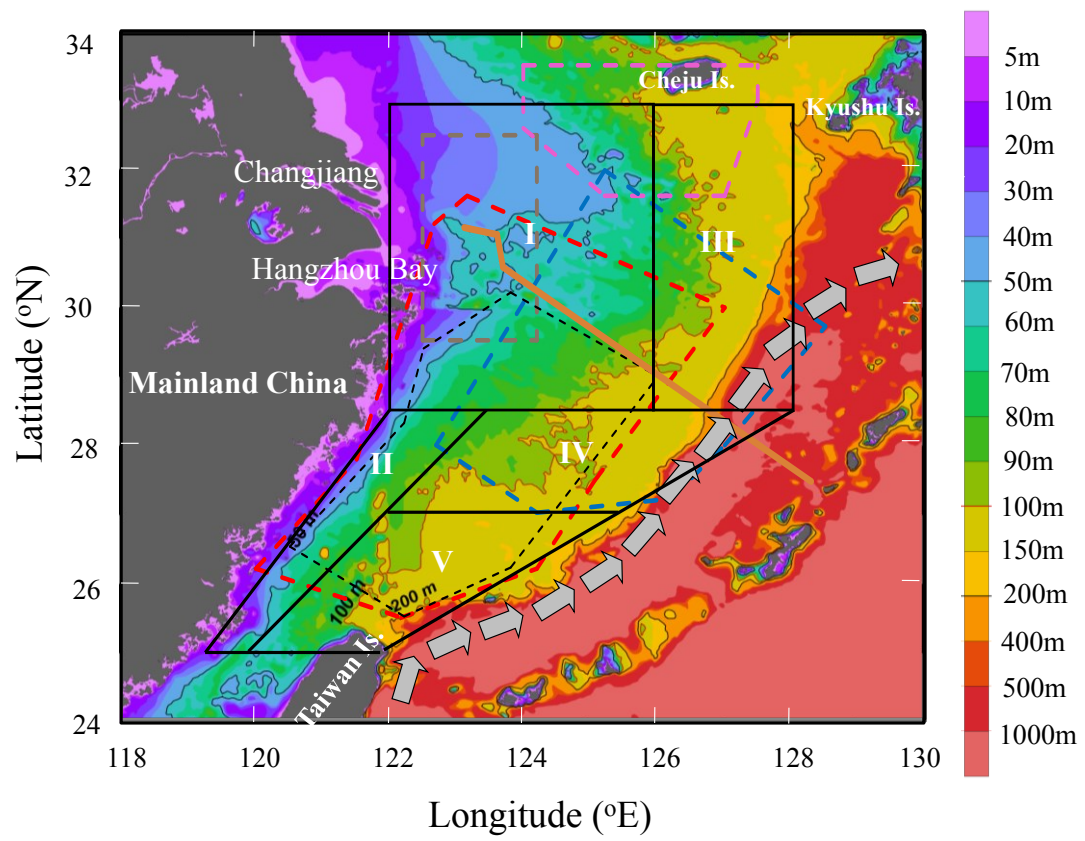
926 November 2010; and the winter surveys include December 2009 and January 2010

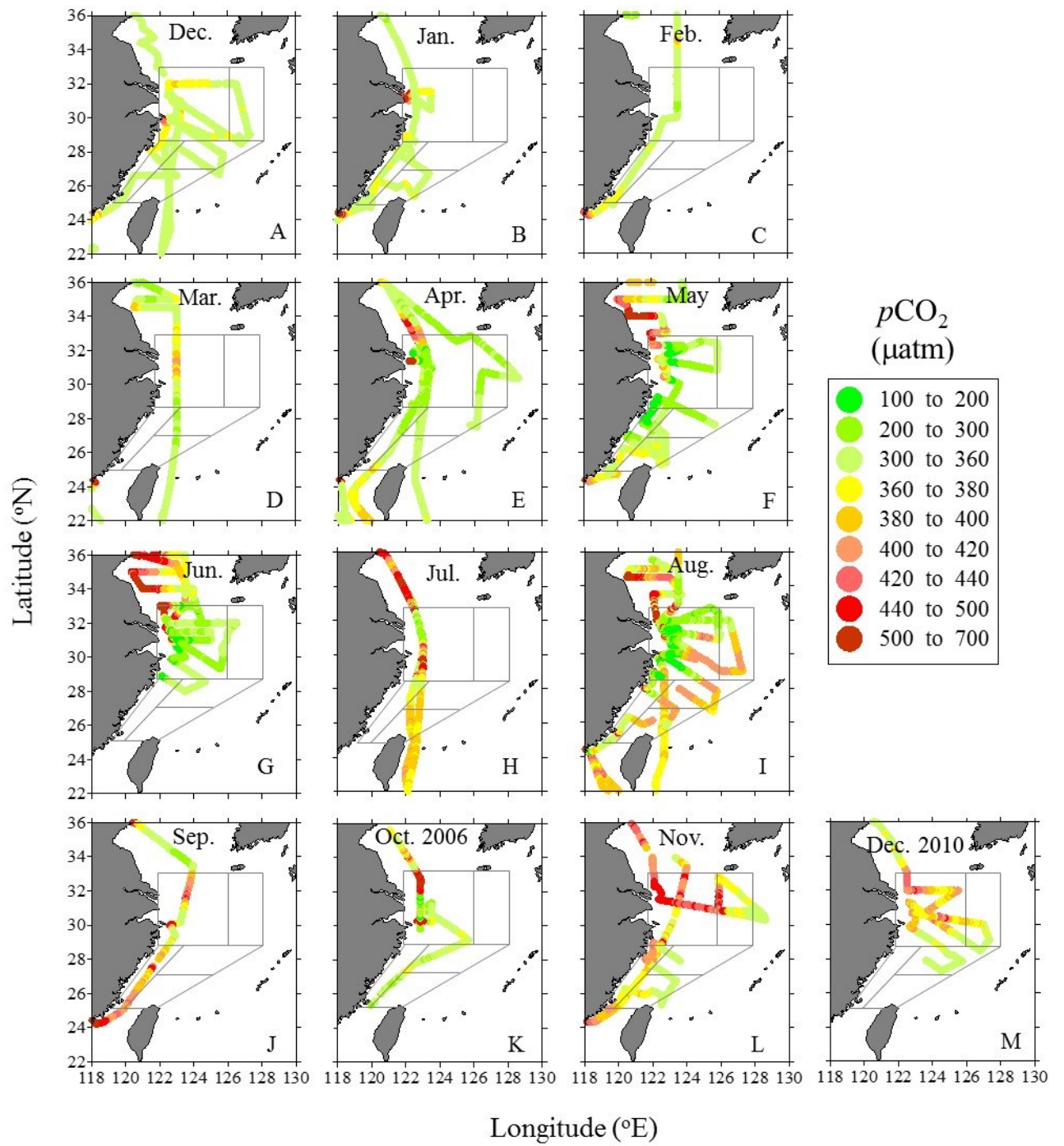
927 surveys. Panels A-1 and B-1 are Domain I; panels A-2 and B-2 are Domain II; panels

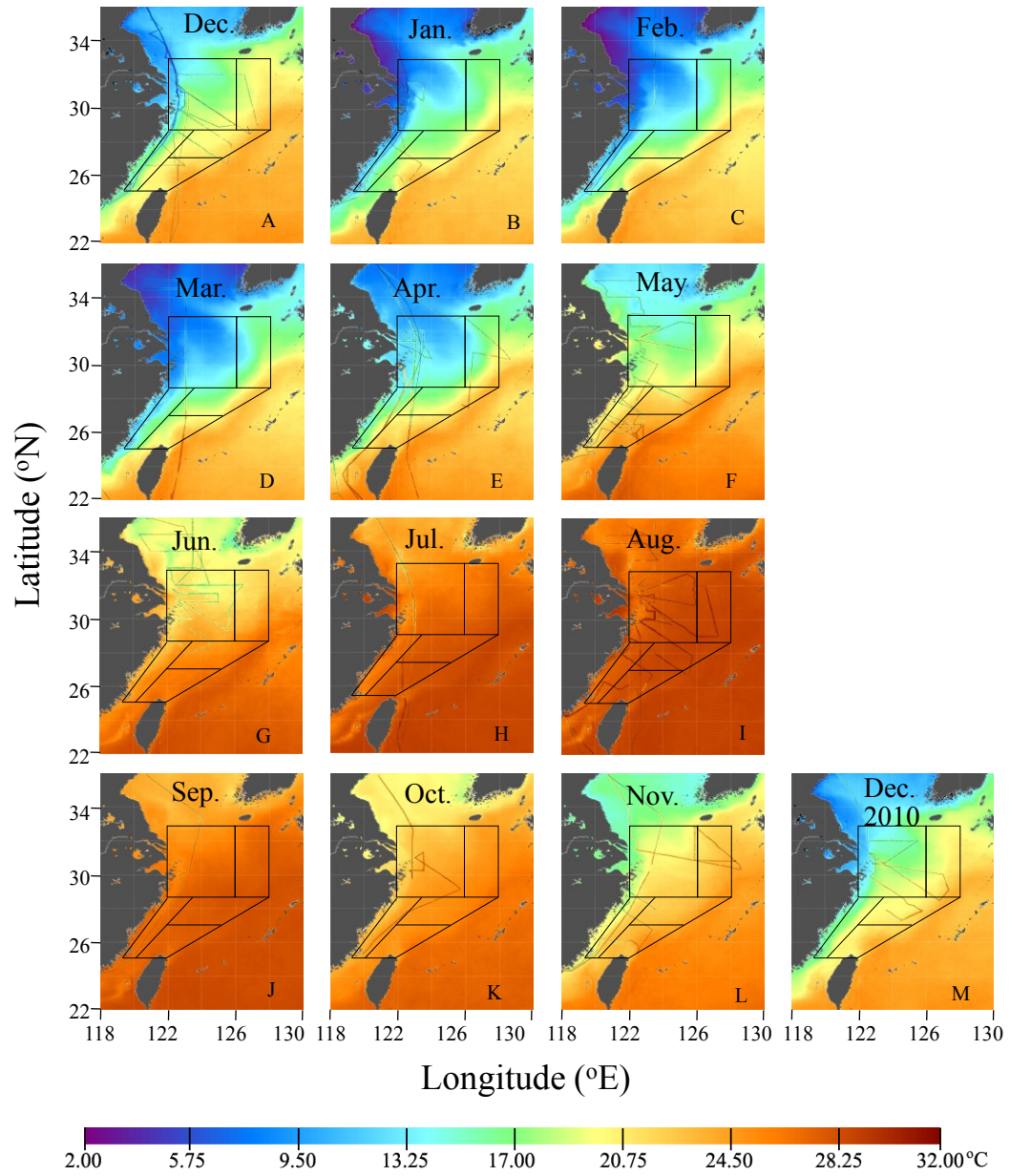
928 A-3 and B-3 are Domain III; panels A-4 and B-4 are Domain IV; panels A-5 and B-5

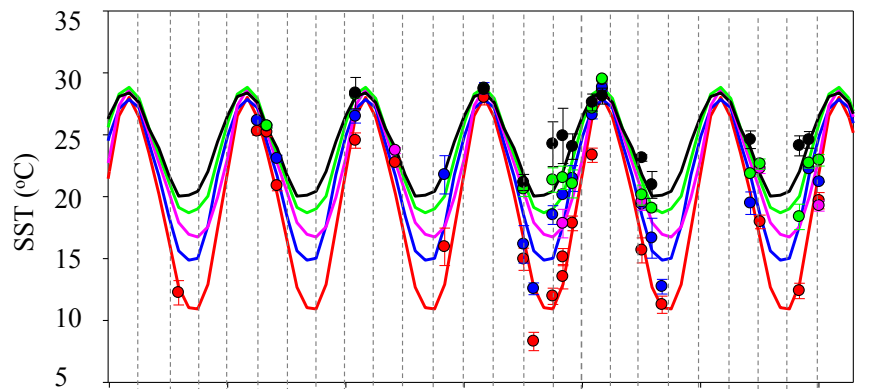
929 are Domain V. $p\text{CO}_2$ and $Np\text{CO}_2$ values are in the year of observations.

930

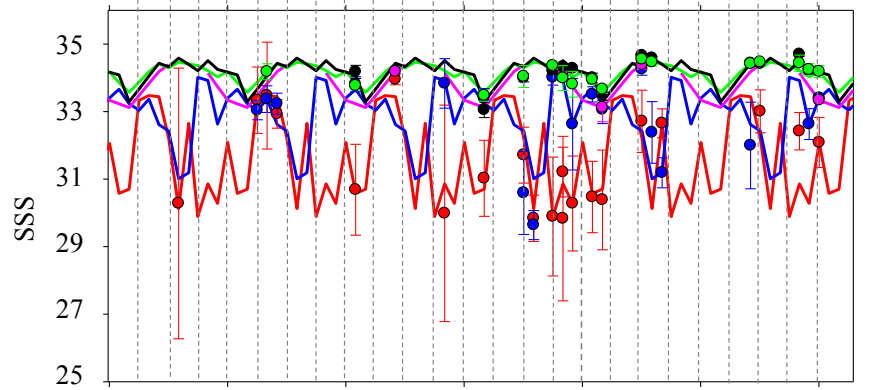
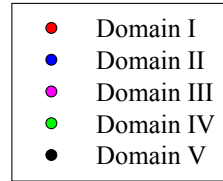








A



B

6 9 12 3 6 9 12 3 6 9 12 3 6 9 12 3 6
 2005 2006 2007 2008 2009 2010 2011
 Observation month

